Modifications of the manuscript "Changes in the geometry and strength of the Atlantic Meridional Overturning Circulation during the last glacial (20-50 ka)".

We would like to thank the reviewers for their constructive comments that helped clarifying our manuscript. Please find below a list of the main changes made to the text and figures, our point by point response to the reviewers (submitted on the 3rd of July 2016), the main text and supplementary material with tracked modifications. Note that the page and line numbering in the list of main modifications refers to the manuscript with tracked changes available below. Thank you for your understanding.

List of main modifications

Main text and figures

P.1, l.21: We replaced the sentences "At the onset of Heinrich Stadial 2, the structure of the AMOC significantly changed. The deep Atlantic was probably directly affected by a southern sourced water mass…" by "Our results further show that during Heinrich Stadial 2, the deep Atlantic was probably directly affected by a southern-sourced water mass…"

P.2, l.5: We replaced the sentence "suggesting that other mechanisms could be required to explain Greenland temperature millennial-scale variability" by "suggesting that Greenland temperature millennial scale variability might be related to more complex changes in Atlantic circulation than simply switching between "on" and "off" circulation modes".

P.2, l.17: We replaced the paragraph "However, interpretation of sedimentary Pa/Th from a single sediment core might be complicated by the non-linear response of Pa/Th to circulation intensity changes (Luo et al., 2010; Thomas et al., 2006). Reconstructing present and past strengths of the AMOC is therefore best achieved by combining Pa/Th records from different water depths and latitudes" by "However, interpretations of sediment Pa/Th from a single core can be ambiguous because similar values can result from different geometry and overturning strength (Luo et al., 2010). Reconstructing past circulation thus requires combining Pa/Th records from multiple sites over a wide range of latitudes and depths".

P.2, l.26: We replaced the sentence "The streamfunctions were simulated with the Earth System model iLOVECLIM under different climatic conditions" by "One streamfunction is derived from present day geostrophic velocity estimates (Talley et al., 2003) and two others were simulated with the Earth System model iLOVECLIM under different climatic conditions".

P.3, l.30: We added the sentence: "Note that because we lack information on past marine productivity changes, we do not account for their potential impact on benthic $\delta^{13}C$ in the present study".

P.4, l.2: We replaced the sentence "sedimentary Pa/Th is a relatively recent tracer that records the renewal rate of water masses occupying the first ~1000 m above the seafloor (Thomas et al., 2006)" by "sedimentary Pa/Th is a relatively recent tracer that can be used to estimate the renewal rate of water masses occupying the first ~1000 m above the seafloor (Thomas et al., 2006, Luo et al., 2010)".

P.5, l.8 and in the entire manuscript and figures: We replaced the term "HS1 streamfunction" by the term "shallow overturning streamfunction".

P.5, l.34: We replaced the paragraph: "The Pa/Th model is a 2D model without parameterization of diffusive transport (Luo et al., 2010). This prevents the model from simulating boundary scavenging, which is the transfer of dissolved protactinium from open ocean regions of high Pa concentrations to coastal regions of low Pa concentration such as in upwelling zones (Christl et al., 2010)" by" The absence of margins in the simple 2D Pa/Th model (Luo et al., 2010) prevents it from simulating boundary scavenging, which is the lateral advection of dissolved Pa from open ocean regions characterized by high Pa concentrations to coastal regions of low Pa concentration such as in upwelling zones (Christl et al., 2010)".

P.6, l.9: We removed the sentence: "Moreover, benthic foraminiferal $\delta^{13}C$ measurements, which reflect the DIC of the water mass directly above the sediment interface, allows confirming or infirming the geometry information contained in measured Pa/Th values".

P.6, l.37: We added the paragraph: "Note that due to the limited number of sedimentary Pa/Th records during MIS3, we can only provide an approximate estimate of water mass boundary positions. Our equatorial transect is however ideally located to record shifts in the position of the transition between southern and northern sourced water masses".

P.9, l.14: We replaced the sentence "the high $d^{13}C$ values of core SU90-03 and MD09-3257 indicate that northern sourced waters were present at ~2500 m in the North and equatorial Atlantic" by "the high $d^{13}C$ values of core SU90-03 and MD09-3257, and low $d^{13}C$ values of core MD02-2594 (< 0.5‰, Negre et al., 2010), indicate that northern sourced waters were present at ~2500 m in the North and equatorial Atlantic".

P.10, l.6: We added the paragraph: "Based on our definition of the Interstadial time slices, we assume that the GI3 time slice reflects interstadial conditions. However, because GI3 seen in Greenland ice cores is of relatively short duration, the Pa/Th signal of the studied sediment cores might not reflect full interstadial circulation conditions. Nonetheless, we consider it unlikely that the Pa/Th of GI3 reflects stadial conditions. Indeed, core MD09-3257 sedimentary Pa/Th values observed during GI3 are similar to those recorded during the GI8 and GI10 time slices that correspond to strict interstadials (Fig. 3)".

Figure 1: A second panel was added to show the position of the sediment cores on a map of the Atlantic Ocean.

Figure 7: This figure was modified to better reflect the uncertainty on the latitudinal and vertical extent of the southern-sourced water mass that we discuss in the text.

Supplementary material

P.1, l.19: We replaced the sentence "Hence, Pa/Th values associated with each time slice on core MD09-3257 are invariant, despite dating uncertainties" by "Hence, Pa/Th values associated with the different time slices in core MD09-3257 are independent from the age model. For all other cores, dating uncertainties account for Pa/Th uncertainties associated with each time slice".

Figure S4: We now display Pa/Th data as a function of opal fluxes in both panels.

Figure S5: We added the coefficient of correlation R^2 next to the linear regression.

Full point by point response to reviewers' comments on manuscript "Changes in the geometry and strength of the Atlantic Meridional Overturning Circulation during the last glacial (20-50 ka)".

We would like to thank the reviewers for their constructive comments. Our point by point response is outlined below. The reviewer's comments are displayed in blue, and our answers are in black and highlighted by asterisks "***". As requested by the editor, we will provide a revised version of the manuscript later in the revision process. Note that page and line numbers that we provide are those associated with the PDF downloaded from http://www.clim-past-discuss.net/cp-2016-26/#discussion. The line numbers the first reviewer provided in the "Technical points" section appear to be different from those that appear on the PDF. Thank you for your understanding.

Referee #1 (Anonymous)

Received and published: 26 May 2016

In their manuscript "Changes in the geometry and strength of the Atlantic Meridional Overturning Circulation during the last glacial (20-50 ka)", Burckel et al. use 231Pa and 230Th ratios and 13C to assess the past state of deep ocean circulation in the Atlantic Ocean at several intervals during the past glaciation. After attempting to assess the geometry and strength of the overturning cell of the Atlantic, they conclude that the deep ocean circulation was very different from the modern in all four of their study intervals. The interstadial circulation was different in being relatively shallow, with a deep inflow from the south. Southward flowing waters at mid-depth would therefore have been the return flow of southern-sourced waters. At the time of Heinrich Stadial 2, yet another different circulation is inferred, with southern waters filling the deep Atlantic and a slow, southward-flowing water mass occupying the intermediate depths.

This is a potentially valuable contribution to the literature on past states of the ocean circulation. It presents new geochemical data in a spatial array that may provide insights into changes at different depths and locations. The isotopic method is a promising and exciting approach, although it seems still in development in comparison to modern measurements. The data are compared to model output, which although limited in resolution and lacking a third dimension, nevertheless provides useful constraints on potential interpretations. The conclusions are not inconsistent with the relatively limited data presented. In terms of the specific criteria, the paper certainly addresses relevant questions within the scope of CP. It does not present novel approaches, but builds well upon existing techniques, data, and ocean modeling output. Substantial conclusions are reached regarding the configuration and rate of ocean circulation. The conclusions are not inconsistent with the data, although there are too many gaps at relevant locations and depths for them to be any more convincing than many alternatives which are not discussed. Figures are relatively clear, and text is a reasonable length. The text is fluent and the authors give adequate credit to the previous studies that they utilize and discuss. The two largest issues with the paper in its present form are related to its justification and chronology.

This is a study of four time slices that are widely distributed within the last glacial. They are neither the most extreme, nor the most characteristic. Nor do they include important transitions or intervals of special climatic interest. It is therefore not clear to the reader why this seemingly arbitrary assortment of time slices was chosen. The authors should provide a much better explanation of the rationale for their selection. It is possibly related to what may be understandable difficulties with a challenging geochemical method, although others, notably Hall, also Negre, McManus, Lippold and Böhm have demonstrated that it is possible to produce continuous highly resolved records of the same isotope systems for specific intervals. Or it may be related to the quality or continuity of the sediment cores. These are acceptable reasons if they are confronted and explained, although it would be most satisfactory if some greater level of scientific rationale were presented. This is currently inadequate, beyond the mention of an interval that was not included. A section of a paragraph or two that would better explain the reasons for the scattered data intervals might seem to the authors to be an acknowledgement of a shortcoming, but in the end it would increase the interest and potential impact of the published study.

*** Pa/Th measurements were focused on relevant MIS3 time slices. HS2 and HS4 in particular were selected because these intervals are characterized by significantly different ice sheet volumes (Lambeck and Chappell, 2001) (see P.2, l.23 of the manuscript). Oceanic circulation around these time periods could therefore reasonably be expected to be different. Unfortunately, it is difficult to disentangle the sedimentary from the oceanic influences on the Pa/Th signal during HS4 in core MD09-3257, as high Pa/Th values are correlated to high ^{232}Th fluxes (Burckel et al., 2015). We therefore focused our study on the time intervals during which the Pa/Th signal of core MD09-3257 can be interpreted in terms of circulation changes, i.e. HS2 and on the DO climate variability encompassing HS2 and HS4. ***

The issue of chronology may be even more crucial, as the authors draw potentially important conclusions about intervals that do not appear to coincide with their data exactly, or in one crucial instance, at all. Figure 3 makes this very clear. None of the shaded intervals truly represent interstadials. The red shaded intervals all cover some portion of one interstadial or another, but the oldest begins at the peak of GI10 and extends beyond the peak of the next stadial, the subsequent shading covers solely a portion of the transition from GI 8 to the next stadial, without including the interstadial peak at all, and the youngest of the three is the only one to cover the entire interstadial GI3, but also includes two times as much duration of full stadial conditions. This does not appear to be just a drafting issue, which might be easily remedied. The shading is well aligned with the sediment data, which largely do not coincide with the ice core evidence.

*** In figure 3, it is clear that every GI (in particular GI10, 8 and 7) is associated with a Pa/Th decrease (i.e. increased circulation intensity). The GI8 and GI10 time slices are well defined as periods of stable oceanic circulation (see section 2.3). Because GI3 is of shorter duration, it is possible that the GI3 time slice does not represent average interstadial conditions, as highlighted page 6, line 10 (see also comments from and answers to Roger François, 2nd reviewer). ***

In the case of the fourth time slice, HS2, the blue shading in Figure 3 aligns well with the new data, until there is an abrupt data gap above the most extreme values, apparently due to a turbidite layer. But the shaded interval is centered on 26 ka, when the published age for HS2 is more than one to two thousand years younger (Naafs et al., 2013, Hodell et al., 2008, Hemming, 2004). Because this interval is well dated, it seems that the new data are older than HS2, which might instead correspond and even be related to the turbidite interval.

*** It is important to distinguish the Heinrich Stadial (defined as the stadial (cold) period during which a Heinrich Event (HE) occurs) and the event itself, characterized by the sedimentary IRD layers. The Pa/Th increase that we observe and that is concurrent with the increase observed in core ODP1063 occurs during GS2, the cold period in the Greenland temperature record during which HE2 is observed in marine sediment cores. ***

A related question is how there appear to be data from this same interval, which is presented as a several thousand year gap in the supplemental figure S2.

*** Turbiditic layers were identified in core MD09-3256Q between 24.16 and 20.88 ka (gap in Figure S2). However, no sedimentary Pa/Th data from this core corresponding to this interval are presented in Figure 3 (last Pa/Th data at 24.16 ka). ***

The authors very reasonably identified intervals of stability in the circulation based on their data, to make the most informative comparison with the model results. These choices did not lead to direct comparisons with the Greenland climate variations, which they accurately describe as important intervals for which the past circulation is not fully or well understood At the very least these chronological issues should be confronted. If they can be adjusted or adequately explained, it will greatly enhance the significance of this study.

*** The fact that oceanic and Greenland signals do not align perfectly could be due to (i)-chronological uncertainties (ii)-real leads or lags of one signal compared to the other (iii)-the response time of geochemical proxies to changes in oceanic circulation. Note that chronological uncertainties were accounted for in calculating the uncertainties associated with the Pa/Th values of each time slice (see supplementary material). ***

Specific comments-

As mentioned in the introduction, the 13C data should have complications due to carbon cycling as well as ocean circulation. These can also be better addressed when interpreting the different time slices, and may help to explain differences in the data not due to circulation.

*** We lack data on changes in marine productivity at the studied sites so we cannot investigate what fraction of the benthic $d^{13}C$ might reflect these changes. We thus follow the classical assumption that $d^{13}C$ reflects changes in bottom water ventilation. We now specify this in section 2.1.1 with the sentence "Note that because we lack information on past marine productivity changes, we do not account for their potential impact on benthic $\delta^{13}C$ in the present study".***

The authors describe an important change at the onset of HS2. Aside from the chronological issues, do they infer that the observed changes relate only to the HS2 interval, or do they establish the LGM condition that is the focus of so many studies?
If it was only during HS2, was the configuration and strength then different from LGM?

*** The change that we observe at the onset of HS2 in core MD09-3257 specifically relates to the HS2 interval, as we observe an increased Pa/Th at the beginning of GS2. Based on Pa/Th and $d^{13}C$ data in cores MD09-3257 and GeoB3910, the onset of the LGM appears to be characterized by an active circulation, however not as active as that of the Holocene. ***

The changes at various depths appear to be under-constrained by the data, in particular because some time slices utilize four sites and others more, but never more than six locations, and no two time slices utilize the same set of locations. This limits the confidence bounds possible in the interpretations, and must allow other consistent alternatives, which should be mentioned and possibly discussed.

*** We agree with reviewer #1's comment and added the following two sentences at the end of section 2.4 to clarify our argumentation: "Note that due to the limited number of sedimentary Pa/Th records during MIS3, we can only provide an approximate estimate of water mass boundary positions. Our equatorial transect is however ideally located to record shifts in the position of the transition between southern and northern sourced water masses." ***

The contrast between the inferred interstadial mode and HS2 mode appears to be related to which direction the waters were moving below 2500 meters. Does that mean that the deep Atlantic was influenced by southern source waters below 2500 in both scenarios?

*** Based on our results, we infer that the Atlantic was likely influenced by southern sourced waters below 2500 m during HS2 but we lack data to determine the precise vertical extent of this southern-sourced water mass. In contrast, during Greenland Interstadials, the transition between southern- and northern-sourced water masses was probably located between 3500 and 2500 m, which would explain the low Pa/Th gradient between our equatorial sediment cores. ***

Many schematic and model representations of the deep Atlantic display a boundary between northern and southern waters that is inclined as a function of latitude. Do the authors consider that also to be possible in their reconstructions?

*** The models representing the deep Atlantic (i.e. streamfunctions, Fig.2, b, d, f), do not display an inclined boundary as a function of latitude. However, the simulated sedimentary Pa/Th (Fig.2, a, c, e) do show increasing sedimentary Pa/Th with latitude along the flow path of any newly formed water mass. We explain this effect page 5 line 11. ***

The presented model shows that boundary to slope deeper to the south in the Holocene, which might suggest that northern waters influence more of the volume of the south Atlantic than the north. Perhaps this can be explained and clarified for those less familiar with this type of geochemical modeling.

*** We are afraid we do not fully understand this question. To render our argumentation accessible to the non-specialized audience, we describe the behavior of dissolved Pa and Th and how this influences the output of the model (see section 2.1.2 and 2.2.1). For a more thorough explanation, we refer the reader to the chapter book by Francois, 2007 (main principles of Pa/Th as a proxy of oceanic circulation intensity) and to the Luo et al., 2010 paper (description of the 2D Pa/Th model). ***

Is the southward flowing mass at intermediate depth GNAIW? Several studies mentioned have inferred a vigourous circulation by this water mass, at least at the LGM. The contrasting conclusion of a sluggish intermediate circulation here is largely based on 13C from the productive equatorial region. Nevertheless, it would be useful to have a more direct discussion in the context of previous interpretations.

*** We make sure not to describe the southward flowing water as GNAIW, as it is indeed defined for the LGM and our study concerns earlier time periods. Our conclusion concerning the sluggish intermediate water mass only relates to HS2. We then see a decrease in Pa/Th (i.e. likely an increase in the overturning intensity) at the onset of the LGM.

Also, we made a few minor changes in order to make clear that we were careful not to over-interpret benthic $d^{13}C$:

P.5, l.28: the sentence "Moreover, benthic foraminiferal $d^{13}C$ measurements, which reflect the DIC of the water mass directly above the sediment interface, allows confirming or infirming the geometry information contained in measured Pa/Th values." was removed.

P.8, l.30: the sentence "the high $d^{13}C$ values of core SU90-03 and MD09-3257 indicate that northern sourced waters were present at ~2500 m in the North and equatorial Atlantic" was changed to "the high $d^{13}C$ values of core SU90-03 and MD09-3257, and low $d^{13}C$ values of core MD02-2594 (< 0.5‰, Negre et al., 2010), indicate that northern sourced waters were present at ~2500 m in the North and equatorial Atlantic".

P.11, l.13: "deep waters likely dominated the deep Atlantic Ocean" was replaced by "deep waters likely filled the deep Atlantic Ocean". We also removed the word "direct" in the sentence : "The direct influence of the southern-sourced water mass likely extended…".

P.11, l.17: we removed "and their associated return flow" from the sentence "…it is difficult to assess the exact position of the southern sourced waters and their associated return flow."

P.11, l.17: we removed the word "directly" in the sentence "This water mass probably directly affected the equatorial Atlantic…".***

Referee #2 (R. Francois)

Received and published: 6 June 2016

Burckel et al combine new and published sediment Pa/Th and benthic d13C data with 2D simulations to assess the strength and geometry of the AMOC during 3 GIs and HS2 They chose these time intervals because they represent time periods with different ice sheet volumes.
Their main conclusions are that AMOC during GIs consisted of a shallow northern overturning cell (likely weaker than the modern NADW) in the upper 2500m, above a deeper southern overturning cell whose volume flow would have been higher than modern AABW. During HS2, as per fig. 3, the circulation geometry stayed the same but was significantly more sluggish.
To me, the take-home message of this study is that the Atlantic overturning circulation during glacial climatic extrema (i.e. Greenland intertadials and Heinrich stadials) had a similar geometry, and were differentiated only by the strength of the overturning cells, with stronger overturning cells during Greenland interstadials and weaker ones during Heinrich stadials. What may be the most surprising here is the apparent stability of AMOC geometry through the glacial period. However, I don't think that circulation contrast between Greenland Interstadials and Greenland (non-Heinrich) Stadials has been clearly documented and discussed in the present manuscript.

General comments
As indicated by the authors, the complete interpretation of sediment Pa/Th will require, to the extent possible, a synoptic database for each time slice of interest. The present study is a valuable contribution towards this end, but I have some questions and comments regarding some details of the interpretation of the data.
Although I recommend "major revisions", I don't think that the revisions I suggest are "major". However, as I am very interested in the topic, I would like to have the opportunity to see the replies of the authors.

Comparing sediment Pa/Th and the Greenland temperature record.
If we accept that abrupt temperature changes in Greenland result from variations in heat transport coinciding with changes in the strength/geometry of the AMOC, one would not expect that changes in sediment Pa/Th would be concurrent with Greenland temperature changes. This is because of the response time of sediment Pa/Th to changes in circulation. For any abrupt change in overturning, the concentration of Pa and Th in the water column will adjust with an e-folding time equivalent to their residence time in the water column (ca. 100-200 y for Pa). It would thus take > 500 y to fully express the change in circulation in sedimentary Pa/Th. This may, in part, address the second question of the other reviewer, at least for GI 8 and 10. I suspect that GI3 may be too brief to yield a measureable Pa/Th signal. On the other hand, if d13C is truly a water mass tracer, then we would expect much less or no lag between the 13C signal and Greenland temperature. However, if decreases in d13C are due to accumulation of nutrients resulting from a sluggish circulation, we would also expect a lag. Another complication when comparing sediment circulation proxies with Greenland temperature is that the latter may also be modulated by the location of the site of deep water formation. Particularly striking is the lack of a Greenland temperature signal at the transition between GS3 and HS2 (as is the case between LGM and HS1).

*** We do not consider $d^{13}C$ as a perfect water mass tracer. The $d^{13}C$ of benthic foraminifera *C. wuellerstorfi* is a proxy of the nutrient content of bottom water masses, that we interpret as reflecting bottom water ventilation. For instance, reduced $d^{13}C$ at a site influenced by northern

sourced waters could result from increased southern sourced water mass influence, or reduced deep water formation in the North Atlantic region.
However, we would like to stress that we are not trying to resolve the timing between changes in deep water circulation and Greenland climate. Timing issues do not alter the interpretation of our time slices, as they are defined based on stable oceanic conditions during Greenland interstadials. ***

In fact, the present manuscript does not address another key question which is whether there are noticeable changes in AMOC between Greenland Stadials and Interstadials (they only contrast Greenland Interstadials and Heinrich Stadials). I would argue that Pa/Th distribution reported to GI3 is mostly a Greenland Stadial signal (because of the brevity of GI3), suggesting no or little changes in AMOC between Greenland Stadials and Interstadials. If this is the case, abrupt changes in Greenland temperature could reflect changes in the site of deep water formation, or northward transport of cooler/warmer surface water. This question could probably be directly addressed with another time slice to the discussion.

*** Because they span different depths on the Brazilian margin, cores MD09-3257 and MD09-3256Q Pa/Th records are particularly interesting to understand the geometry and strength of the AMOC during MIS3. Unfortunately we lack data in core MD09-3256Q during Greenland stadials. We therefore decided not to define stadial time slices. However, as we point out page 6, line 10, we agree that GI3 time slice might not reflect interstadial conditions. We have therefore added the following short paragraph (inserted P.9, l.20) to explain that this time slice may reflect stadial conditions and discuss the implications: "Based on our definition of Interstadial time slices, we assume that the GI3 time slice reflects interstadial conditions. However, because GI3 seen in Greenland ice cores is of relatively short duration, the Pa/Th signal of the studied sediment cores might not reflect full interstadial circulation conditions. Nonetheless, we consider it unlikely that the Pa/Th of GI3 reflects stadial conditions. Indeed, core MD09-3257 sedimentary Pa/Th values observed during GI3 are similar to those recorded during the GI8 and GI10 time slices that correspond to strict interstadials (Fig. 3).". ***

Additional comments
Abstract; Line 21: "At the onset of HS2, the structure of the AMOC significantly changes" "Structure" is too vague a term. I think it is worth highlighting here that the present data set is interpreted to indicate that the geometry of the overturning circulation did not change (as per Fig. 7) but circulation was much weaker.

*** While this is indeed a possibility, we do not conclude that the geometry of the AMOC did not change between Heinrich Stadial 2 and Greenland Interstadials. We cannot say if the southern sourced water mass influence extended above 2500 m during HS2 (page 11, line 13). We removed the term structure and wrote "during Heinrich Stadial 2, the deep Atlantic was probably directly affected by a southern-sourced water mass". ***

P2; line 4-5: ".. suggesting that other mechanisms could be required to explain Greenland temperature millennial scale variability" The accepted mechanism is heat transport by the AMOC. The presence of a shallow circulation cell during HS is not inconsistent with this mechanism and does not require an alternative explanation.

*** We agree with your point and therefore chose to use the terms "could be required". In order to clarify the text, we modified the sentence as follows "… suggesting that Greenland temperature millennial scale variability might be related to more complex changes in Atlantic circulation than simply switching between "on" and "off" circulation modes." ***

P2; line 14 – 15: I would suggest: However, interpretation of sediment Pa/Th from a single core can be ambiguous because similar values can result from different geometry and overturning strength (Luo et al., 2010). Reconstructing past circulation thus requires combining Pa/Th records from multiple sites over a wide range of latitudes and depths (refs).

*** Your suggestion makes the issue of interpreting a single core clearer by pointing the possibility of having multiple circulation intensities for a single sedimentary Pa/Th value. We modified the sentence following your suggestion. ***

P2; line 22: I would suggest: The streamfunction under Heinrich Stadial conditions* were simulated with the Earth System model Iloveclim (ref) while the Holocene streamfunction was derived from geostrophic velocity estimates (ref) *later on, this is becoming confusing, since the HS simulation does not fit the HS data..

*** We changed the sentence to:
"One streamfunction is derived from present day geostrophic velocity estimates (Talley et al., 2003) and two others were simulated with the Earth System model iLOVECLIM under different climatic conditions (Roche et al., 2014)."
As described below, we agree with your comment on the confusing nature of the terminology used and changed "HS1 streamfunction" into "Shallow overturning streamfunction". ***

P3; line 6 – 8: This should be moved to section 2.1.2.

*** Although we understand the potential issue of mentioning Pa/Th in the "Sediment cores" section, we prefer to group all cores at the beginning of the paper for the sake of clarity. ***

I note that the South Atlantic record of Jonkers et al is not mentioned. Is it because this core sedimentation rate is to low? It would still be worth checking if their glacial values are consistent with the AMOC scenarios presented here.

*** Unfortunately, none of Jonkers et al.'s Pa/Th data are within our time slices. However, the low sedimentary Pa/Th values that they describe fit very well with our assumptions of intensified deep water formation in the South Atlantic (it would help to systematically exclude the Holocene streamfunction). ***

P3; line 34: "Pa/Th records renewal rates of water masses ca. 1000m above the seafloor" While it is correct that sediment Pa/Th records Pa and Th scavenging mostly coming from the water ca. 1000m above the seafloor, it does not record renewal rates of this water mass. The scavenging of Pa and Th from this water mass is in part controlled by its Pa and Th concentration, which is influenced by the overall geometry and strength of the AMOC. That is why, as indicated by the authors, interpretation of sediment Pa/Th requires a synoptic database for each time slice of interest.

*** We agree that the sentence: "Pa/Th is a relatively recent tracer that records the renewal rate of water masses occupying the first ~1000 m above the seafloor (Thomas et al., 2006)" could be misleading and we replaced it by "Pa/Th is a relatively recent tracer that can be used to estimate the renewal rate of water masses occupying the first ~1000 m above the seafloor (Thomas et al., 2006, Luo et al., 2010)". ***

P3; line 40 I suggest "High (low) rate of overturning" rather than "High (low) flow rates.."If circulation was only horizontal and scavenging intensity uniform in the ocean, sediment Pa/Th would not be dependent on flow rate

*** We agree that overturning is indeed required for sedimentary Pa/Th. We changed the sentence following your suggestion. ***

P5; line 13: I would suggest: ..Pa/Th increases along the flow path of any newly-formed deep water masses*, as initially low dissolved Pa concentrations increase: : : *it is not true that Pa/Th increase along the flow path of any water mass.

*** We agree and changed the sentence following your suggestion. ***

P5; line 18-19: While there is no explicit parameterization of diffusive transport in the 2D model, it is present in the model and it is controlled by horizontal velocities and horizontal grid spacing. In the model used by Luo et al., the inherent mixing is about 800ms□2, which is in the upper range of the along-isopycnal tracer diffusivities. Therefore, it is not the lack of diffusive transport that prevents the model from simulating boundary scavenging. Instead, it is simply because it is a 2D model and there are no margins. Including boundary scavenging at ocean margins would require a 3D model (or an open 2D model).

*** Thank you very much for your input concerning the 2D Pa/Th model. We changed the paragraph into the following: : "The absence of margins in the simple 2D Pa/Th model (Luo et al., 2010) prevents it from simulating boundary scavenging, which is the transfer of dissolved protactinium from open ocean regions of high Pa concentrations to coastal regions of low Pa concentration such as in upwelling zones (Christl et al., 2010). However, as described in the results section, we verified that our Pa/Th signal is mainly driven by oceanic circulation changes and the importance of diffusive transport is therefore likely negligible here. This simple 2D Pa/Th model therefore appears adequate for comparison with our Pa/Th data." ***

P5; line 21 – 22: Boundary scavenging is weak in the Holocene Atlantic because of the short residence time of deep water in this basin (which results from a high overturning rate). This may not be the case for Heinrich Stadials and the expression of boundary scavenging at the margins during these events would depend on their duration. If the ocean stays in its Heinrich Stadial mode long enough (500 – 1000 years?) to start expressing boundary scavenging, the 2 D model will overestimate the Pa/Th in cores located in low productivity central basin regions and underestimate the Pa/Th in cores located at the margin. This needs to be kept in mind when interpreting the data

*** See below for answers concerning these concerns. ***

P5; line 35: As discussed above, if their duration is long enough, boundary scavenging should be expressed during Heinrich Stadials (if they are characterized by a very sluggish AMOC). If it is expressed during H4 but not during H2, this is an observation that needs discussion (was AMOC more sluggish during HS4? Was HS2 a briefer event? These questions should at least be raised). On the other hand, based on Fig. 3, it seems that boundary scavenging was also expressed during HS2 (as we would expect..)

*** Yes, we indeed have boundary scavenging during HS2, e.g. indicated by sedimentary Pa/Th ratios above the Pa/Th production ratio. However, we showed in a previous study that changes in sedimentary Pa/Th are mainly driven by oceanic circulation changes in core MD09-3257 (Burckel et al., 2015). On the contrary, HS4 Pa/Th values in core MD09-3257 appear to be mostly driven by vertical terrigenous fluxes (Burckel et al., 2015). We therefore chose to exclude these values (open squares in Fig. 3) and HS4 when discussing oceanic circulation. ***

Fig. 1: I suggest adding a panel showing long/lat of the cores to make it easier to visualize how boundary scavenging could affect Pa/Th in each core

*** We agree with your comment, but table S1 already lists the cores' positions and depths, along with the age models used. We therefore prefer to add a second panel to Figure 1 to show the position of all cores in the Atlantic Ocean. ***

Fig. 3 caption: I don't understand "average Pa/Th for each core is represented by the lines"

*** We mean "Replicates averaged Pa/Th signal". We modified the sentence: "In (a) the average Pa/Th for each core is represented by the lines and individual measurements by diamonds or squares (MD09-3257)." into "In (a) lines pass through average Pa/Th values in case of replicates, while diamonds and squares (MD09-3257) correspond to individual Pa/Th measurements". ***

P6; line 21: I would remove "indicating the absence of Pa export" Instead, Pa/Th > 0.093 indicates the influence of boundary scavenging in this margin core. We wouldthen expect that the 2D model underestimate the measured Pa/Th. Likewise, we would expect that Pa/Th measured in open ocean cores during that time would be lower than those generated by the model.

*** We would like to keep this sentence, as high Pa/Th signal at that time is reflecting reduced overturning rates. If we were to write "indicating boundary scavenging", we fear that the reader might think that sedimentary processes are overprinting the oceanic circulation information.
Moreover, because reduced Atlantic basin width at the latitude of our Brazilian sites could result in an overestimation of simulated sedimentary Pa/Th (Lippold et al., 2011, see p.9, l.33 of the manuscript), the underestimation of sedimentary Pa/Th due to the absence of boundary scavenging in the 2D model might be partially or totally compensated on the North Brazilian margin. ***

P6; line 22: "Pa/Th variability associated with GS and GI is observed" Pa/Th for GI 10, 8 and HS2 (and 4; I am not sure why HS4 is not considered in the discussion; boundary scavenging is also apparent during HS2) are well documented. If the authors want to discuss AMOC variability between GS and GI, however, they need to add and discuss another time slice corresponding to a GS (same remark for p7; line 19)

*** Although there seems to be a difference between GI and GS oceanic circulation based on core MD09-3257 Pa/Th record we do not want to discuss variability between GS and GI because we lack a more comprehensive picture of the circulation during GS due to the absence of Pa/Th data in core MD09-3256Q during these periods. ***

Section 4.2.1 GI data fit well with the HS1 simulation (particularly is the latitude of deep water formation is adjusted). On the other hand, HS2 data do not fit well with HS1 simulation. This is confusing. If we accept the interpretation of the HS2 data, that would mean that the so-called HS1 simulation does not simulate circulation during Heinrich Stadials. Shouldn't then this simulation be called something else? (e.g. shallow, moderate overturning circulation scheme or such). What is the basis for taking the "HS1" streamfunction as representative of Heinrich Stadial circulation?

*** The names of the streamfunctions originate from the paper of Roche et al., 2014. The HS1 streamfunction is generated with a 0.16 Sv freshwater forcing in the Labrador Sea and allows for the presence of a shallow overturning cell, while a 0.35 Sv forcing results in the absence of deep-water formation in the high latitude North Atlantic (off-mode).
However, we agree that calling one of the streamfunctions HS1 is confusing, especially when compared to the HS2 time slice. We therefore renamed this streamfunction "Shallow overturning streamfunction" in the entire manuscript. ***

P11; line 33: "Our data shows that the geometry of the AMOC changed at the onset of HS2" As illustrated on Fig. 7, the geometry did not change, only the rate of volume transport changed.

*** You are right, we modified "changed" into "likely changed". Based on our data we cannot determine the exact vertical extent of the southern sourced water mass on the Brazilian margin. We also modified Fig. 7 in order to picture the uncertainty on the vertical extent of the southern sourced water mass in the HS2 time slice. ***

S2 (Pa/Th uncertainties) I don't understand the meaning of "Hence, Pa/Th values associated with each time slice on core MD.. is invariant, despite dating uncertainties"

*** Because time slices are defined based on MD09-3257 Pa/Th signal, age uncertainties do not affect Pa/Th uncertainties associated with each time slice in this core. For all other cores, age uncertainties affect the Pa/Th uncertainties associated with each time slice. This has been clarified in the text. The new sentence reads: "Hence, Pa/Th values associated with the different time slices in core MD09-3257 are independent from the age model. For all other cores, dating uncertainties account for Pa/Th uncertainties associated with each time slice." ***

Changes in the geometry and strength of the Atlantic Meridional Overturning Circulation during the last glacial (20-50 ka)

Pierre Burckel[1], Claire Waelbroeck[1], Yiming Luo[2], Didier M. Roche[1,3], Sylvain Pichat[4], Samuel L. Jaccard[5], Jeanne Gherardi[1], Aline Govin[1], Jörg Lippold[5], François Thil[1]

[1]Laboratoire des Sciences du Climat et de l'Environnement, LSCE/IPSL, CEA-CNRS-UVSQ, Université Paris-Saclay, F-91191 Gif-sur-Yvette, France

[2]Dalhousie University, Department of Oceanography, 1355 Oxford Street, PO BOX 15000, Halifax, NS B3H 4J1, Canada

[3]Department of Earth Sciences, Earth and Climate Cluster, Faculty of Earth and Life Sciences, Vrije Universiteit Amsterdam, Amsterdam, The Netherlands

[4]Laboratoire de Géologie de Lyon (LGL-TPE), Ecole Normale Supérieure de Lyon, 46 allée d'Italie, 69007 Lyon, France

[5]Institute of Geological Sciences and Oeschger Centre for Climate Change Research, University of Bern, Baltzerstr. 1+3, CH-3012, Bern, Switzerland

Correspondence to: Pierre Burckel (pierre.burckel@lsce.ipsl.fr)

Abstract. We reconstruct the geometry and strength of the Atlantic Meridional Overturning Circulation during Heinrich Stadial 2 and three Greenland interstadials of the 20-50 ka period based on the comparison of new and published sedimentary $^{231}Pa/^{230}Th$ data with simulated sedimentary $^{231}Pa/^{230}Th$. We show that the deep Atlantic circulation during these interstadials was very different from that of the Holocene. Northern-sourced waters likely circulated above 2500 m depth, with a flow rate lower than that of the present day North Atlantic Deep Water (NADW). Southern-sourced deep waters most probably flowed northwards below 4000 m depth into the North Atlantic basin, and then southwards as a return flow between 2500 and 4000 m depth. The flow rate of this southern-sourced deep water was likely larger than that of the modern Antarctic Bottom Water (AABW). Our results further show that during~~At the onset of~~ Heinrich Stadial 2, the ~~structure of the AMOC significantly changed. The~~ deep Atlantic was probably directly affected by a ~~southern~~ southern-sourced water mass below 2500 m depth, while a slow southward flowing water mass originating from the North Atlantic likely influenced depths between 1500 and 2500 m down to the equator.

1 Introduction

Greenland ice core records show that the last glacial climate repeatedly shifted between cold (stadial) and warm (interstadial) conditions (Johnsen et al., 1992). Greenland Stadials (GS) and Greenland Interstadials (GI) are the Greenland expressions of the characteristic millennial-scale Dansgaard-Oeschger events that represent cold and warm phases of the North Atlantic region, respectively (Rasmussen et al., 2014). GS typically lasted for several centuries, and were followed by a rapid warming of up to 15°C achieved in at most a couple of centuries (Kindler et al., 2014). The subsequent GI then lasted for several centuries to millennia, with Greenland temperatures slowly decreasing and leading to the onset of a new GS. During some of the GS, icebergs were released from high latitude northern hemisphere ice sheets into the North Atlantic Ocean, and their melting led to the deposition of ice rafted detritus on the seafloor, as observed in marine sediment cores (Heinrich, 1988). We refer to these periods as Heinrich Stadials (HS).

Changes in Atlantic Ocean circulation have long been suggested to impact Greenland temperatures (Broecker et al., 1985) and could be at the origin of the glacial millennial-scale variability. Indeed, there is much evidence for decreased North Atlantic deep-water formation and increased influence of southern-sourced deep waters in the Atlantic during Heinrich Stadials (Elliot et al., 2002; McManus et al., 2004; Skinner et al., 2003; Vidal et al., 1997). Moreover, climate models are able to reproduce the bipolar seesaw pattern characterizing millennial-scale glacial variability through variations of the strength of the Atlantic Meridional Overturning Circulation (AMOC) in response to freshwater forcings (Ganopolski and Rahmstorf, 2001). However, recent studies show that a shallow circulation cell could have been still active during HS (Bradtmiller et al., 2014; Gherardi et al., 2009; Lippold et al., 2016; Lynch-Stieglitz et al., 2014; Roche et al., 2014; Wary et al., 2015), suggesting that Greenland temperature millennial scale variability might be related to more complex changes in Atlantic circulation than simply switching between “on” and “off” circulation modes~~other mechanisms could be required to explain Greenland temperature millennial-scale variability~~. A better understanding of the vertical layout and flow rate of the water masses constituting the AMOC during the last glacial is therefore needed to assess the relationship between AMOC and glacial millennial-scale variability.

Sedimentary $(^{231}Pa/^{230}Th)_{xs,0}$ (activity ratio of ^{231}Pa and ^{230}Th unsupported by lithogenic and authigenic uranium and corrected from decay to the time of sediment deposition, Pa/Th hereafter) records were first used to assess the AMOC intensity during the Last Glacial Maximum (LGM) (Yu et al., 1996). Since then, Pa/Th records have been used in the Atlantic to infer changes in the intensity of the deep ocean circulation during HS (Böhm et al., 2015; Bradtmiller et al., 2014; Burckel et al., 2015; Gherardi et al., 2005, 2009; Henry et al., 2016; McManus et al., 2004; Lippold et al., 2016). The comparison of simulated sedimentary Pa/Th values with core top Pa/Th data has shown that sedimentary Pa/Th reflects circulation intensity in the modern Atlantic Ocean (Lippold et al., 2011).

However, interpretations of sediment Pa/Th from a single core can be ambiguous because similar values can result from different geometry and overturning strength (Luo et al., 2010). Reconstructing past circulation thus requires combining Pa/Th records from multiple sites over a wide range of latitudes and depths~~However, interpretation of sedimentary Pa/Th from a single sediment core might be complicated by the non-linear response of Pa/Th to circulation intensity changes (Luo et al., 2010; Thomas et al., 2006). Reconstructing present and past strengths of the AMOC is therefore best achieved by combining Pa/Th records from different water depths and latitudes~~ (Gherardi et al., 2009; Lippold et al., 2011, 2012, 2016).

In this study, we present new sedimentary Pa/Th data from a deep sediment core recovered from the Brazilian margin, and from an intermediate depth core from the mid-latitude North Atlantic. We then compare last glacial Pa/Th records from different water depths and latitudes with Pa/Th values simulated using a simple 2D box model (Luo et al., 2010) forced by various streamfunctions. One streamfunction is derived from present day geostrophic velocity estimates (Talley et al., 2003) and two others were simulated with the Earth System model iLOVECLIM under different climatic conditions (Roche et al., 2014).~~The streamfunctions were simulated with the Earth System model iLOVECLIM under different climatic conditions (Roche et al., 2014).~~ Results of this comparison allow us to constrain the geometry and strength of the AMOC during GI-3, -8, -10 (Rasmussen et al., 2014) and HS2. We chose to focus our study on HS2 and the interstadials surrounding HS2 and HS4 as these periods are associated with very different ice-sheet volumes (Lambeck and Chappell, 2001).

2 Material and methods

2.1 Sediment cores

Sediment cores MD09-3257 (04°14.69’S, 36°21.18’W, 2344 m water depth) and MD09-3256Q (03°32.81’S, 35°23.11’W, 3537 m water depth) were recovered from the Brazilian margin during R/V Marion Dufresne cruise MD173/RETRO3 (Fig. 1). Improved recovery of deep-sea sediments with no or little deformation of sediment layers was achieved during this coring cruise thanks to the systematic use of the CINEMA software (Bourillet et al., 2007; Woerther and Bourillet, 2005). This software computes the amplitude and duration of the elastic recoil of the aramid cable, and the piston displacement throughout the coring phase, accounting for the length of the cable (water depth) and total weight of the coring system. The length of the coring cable is indeed of primary importance regarding the deformation rate of the 'Calypso' long piston cores (Bourillet et al., 2007; Skinner and McCave, 2003).

Core GeoB3910 (04°14.7'S, 36°20.7'W, 2362 m water depth) (Jaeschke et al., 2007) was recovered from approximately the same position and depth as core MD09-3257, during Meteor cruise M34/4. Hereafter we refer to both GeoB3910 and MD09-3257 as intermediate equatorial cores and to MD09-3256Q as the deep equatorial core. At present, the Brazilian margin at these depths is bathed by the North Atlantic Deep Water (NADW) (Fig. 1). Because the Brazilian margin is affected by western boundary currents (Rhein et al., 1995), these sediment cores are ideally located to observe changes in the strength and extent of the intermediate and deep AMOC water masses (Schott, 2003).

Sediment core SU90-03 (40°30.3'N, 32°3.198'W, 2475 m) was recovered from the northern margin of the subtropical gyre (Chapman et al., 2000). Its location in the mid-latitude North Atlantic provides information on changes in NADW production rates that could not be deduced from the sole equatorial depth transect.

We compare these Pa/Th records with published records from other Atlantic cores that span the 20-50 ka period: ODP Leg 172 site 1063 (33°41'N, 57°37'W, 4584 m, ODP1063 hereafter) (Böhm et al., 2015), MD02-2594 (34°43'S, 17°20'E, 2440 m) (Negre et al., 2010) and V29-172 (33°42'N, 29°22.98'W, 3457 m) (Bradtmiller et al., 2014) (Fig. 1, Table S1).

2.1.1 Benthic δ13C

The stable carbon isotopic composition ($\delta^{13}C$) of the epifaunal benthic foraminifer *Cibicides wuellerstorfi* has been shown to record the $\delta^{13}C$ of bottom-water dissolved inorganic carbon (DIC) with minor isotopic fractionation (Duplessy et al., 1984; Zahn et al., 1986). Initial DIC isotopic concentration is acquired by a water mass in its formation region by surface productivity (which consumes ^{12}C therefore increasing dissolved $\delta^{13}C$) and temperature dependent air-sea interactions (Lynch-Stieglitz et al., 1995; Rohling and Cooke, 2003). DIC $\delta^{13}C$ then evolves as deep water ages, because the constant export of ^{12}C-enriched biogenic material that is remineralized at depth leads to the decrease of the DIC $\delta^{13}C$ along the flow path of the water mass. As DIC $\delta^{13}C$ largely follows water mass structure and circulation in the modern ocean, *C. wuellerstorfi* $\delta^{13}C$ has been used to trace water masses, with a decrease in *C. wuellerstorfi* $\delta^{13}C$ being interpreted as a decrease in bottom water ventilation, and conversely (e.g. Duplessy et al., 1988). However, the information on bottom water ventilation embedded in *C. wuellerstorfi* $\delta^{13}C$ is complicated by the impact of changes in surface water $\delta^{13}C$, marine biological productivity and continental biomass changes.

Because LGM $\delta^{13}C$ values are higher in ~~northern~~ northern-sourced waters (1.5 ‰) than in ~~southern~~ southern-sourced waters (<-0.2 ‰)(Curry and Oppo, 2005), we interpret a decrease in *C. wuellerstorfi* $\delta^{13}C$ values at the equatorial sites as an increase in the time elapsed since the water mass was last in contact with the atmosphere or as an increased influence of nutrient-rich ~~southern~~ southern-sourced deep waters. Note that because we lack information on past marine productivity changes, we do not account for their potential impact on benthic $\delta^{13}C$ in the present study.

Core MD09-3256Q benthic foraminifer *C. wuellerstorfi* were handpicked in the size fraction higher than 250µm, washed with methanol in an ultrasonic bath, and then roasted in glass vials at 380°C under vacuum for 45 min. *C. wuellerstorfi* $\delta^{13}C$ (expressed in ‰ VPDB) was measured at LSCE (Gif-sur-Yvette) using an Elementar Isoprime mass spectrometer. VPDB is defined with respect to NBS-19 calcite standard ($\delta^{18}O$ = -2.20 ‰ and $\delta^{13}C$ = +1.95 ‰) (Coplen, 1988). The mean external reproducibility (1σ) of carbonate standards is ± 0.05 ‰ for $\delta^{18}O$ and ± 0.03 ‰ for $\delta^{13}C$. Measured NBS-18 $\delta^{18}O$ is -23.2 ± 0.2 ‰ VPDB and $\delta^{13}C$ is -5.0 ± 0.1 ‰ VPDB. $\delta^{13}C$ measurements were done at the highest possible resolution, depending on the availability of C. *wuellerstorfi* (usually every 1 to 2 cm).

2.1.2 Sedimentary Pa/Th

In contrast to *C. wuellerstorfi* $\delta^{13}C$, which reflects the nutrient content of bottom waters, sedimentary Pa/Th is a relatively recent tracer that can be used to estimate the renewal rate of water masses occupying the first ~1000 m above the seafloor (Thomas et al., 2006, Luo et al., 2010)~~sedimentary Pa/Th is a relatively recent tracer that records the renewal rate of water masses occupying the first ~1000 m above the seafloor (Thomas et al., 2006)~~. This tracer has been successfully used to reconstruct past changes in deep Atlantic circulation intensity (Böhm et al., 2015; Gherardi et al., 2005, 2009; Guihou et al., 2010, 2011; Hall et al., 2006; Henry et al., 2016; Jonkers et al., 2015, Lippold et al., 2011, 2012; 2016, McManus et al., 2004, Negre et al., 2012; Yu et al., 1996).

^{231}Pa and ^{230}Th are produced at a constant Pa/Th activity ratio of 0.093 by dissolved uranium, which is homogeneously distributed in the oceans. ^{230}Th is however much more particle reactive than ^{231}Pa, as reflected by their respective residence time in the ocean (30-40 y for ^{230}Th, 200 y for ^{231}Pa, Francois, 2007). ^{230}Th is therefore rapidly removed from the water column to the underlying sediment, while ^{231}Pa can be advected by oceanic currents. High (low) ~~flow~~ rates of overturning therefore result in high (low) ^{231}Pa export and hence low (high) sedimentary Pa/Th ratio in the Atlantic. However, affinities of ^{231}Pa and ^{230}Th for settling particles depend on the particle type (Chase et al., 2002). For instance, ^{231}Pa has a high affinity for opal, so that high opal fluxes can result in high sedimentary Pa/Th values even in the presence of lateral advection (Chase et al., 2002). The origin of sedimentary Pa/Th variability therefore needs to be carefully assessed.

Pa/Th measurements on core MD09-3256Q were performed by isotopic dilution mass spectrometry on a Thermo Finnigan MC-ICP-MS Neptune, following the method of Guihou et al., 2010.

Core SU90-03 sedimentary Pa/Th was measured by isotopic dilution on a single collector, sector field ICP-MS (Element2) at the University of British Columbia, following the procedure described by Choi et al., 2001.

For both cores, Pa and Th are corrected from radioactive decay since the time of sediment deposition and from authigenic and lithogenic components using a $^{238}U/^{232}Th$ ratio of 0.5±0.1 (Fig. S1) (Guihou et al., 2010).

2.1.3 Age model

Over the period 0-34 ka, core MD09-3256Q age model is based on 11 ^{14}C dates measured on planktic foraminifer *G. ruber* white and converted to calendar age using the Marine13 curve with no additional reservoir age correction (Reimer et al., 2013) (Fig. S2). During the last glacial, Heinrich Stadials were recorded in marine sediment cores from the Brazilian margin as Ti/Ca peaks resulting from increased terrigenous input during periods of increased precipitation associated with southward shifts in the position of the Inter Tropical Convergence Zone (ITCZ) (Jaeschke et al., 2007). Ti/Ca peaks are therefore good stratigraphic markers for correlating sediment cores with neighbouring well-dated cores. Therefore, from 34 ka to 50 ka, core MD09-3256Q was dated by correlation of its Ti/Ca record with that of core GeoB3910 using two tie points corresponding to the Ti/Ca peaks associated with HS4 and -5. The GeoB3910 age model over the 34 to 50 ka period is based on one ^{14}C date calibrated using the Marine13 curve and on four speleothem tie points at the onset and end of HS4 and 5 (Burckel et al., 2015). Core MD09-3256Q age model and sedimentation rates are given in Table S2 and Fig. S3. The age model of core SU90-03 is based on 17 ^{14}C dates measured on various species of planktic foraminifera (Chapman et al., 2000) that were converted to calendar ages using Marine13 calibration curve with no additional reservoir age correction.

^{14}C dates of all the published Atlantic cores used in this study were converted into calendar ages using the same method (Table S1).

2.2 Circulation and Pa/Th model

2.2.1 Description of the models

In order to assess the vertical layout and renewal rate of the water masses constituting the AMOC during the last glacial period, the sedimentary Pa/Th data of the studied sediment cores were compared to Pa/Th values simulated with a simple 2D box model (Luo et al., 2010) forced by different streamfunctions (Fig. 2b, d, f). Streamfunctions were generated using the iLOVECLIM coupled climate model, comprising atmosphere, ocean and vegetation components (Roche et al., 2014). A LGM equilibrium state computed using the PMIP-2 protocol was used as background climate (see Roche et al., 2007) for details). Streamfunctions ~~used to mimic~~characterized by a shallow (<2500 m) northern sourced overturning cell (shallow overturning streamfunction) ~~HS1~~ and by a complete shutdown of the AMOC (off-mode streamfunction) were generated by imposing a 0.16 and 0.35 Sv freshwater forcing in the Labrador Sea, respectively (Roche et al., 2010, 2014). The freshwater input is added during 300 years on the LGM background state. The streamfunctions are taken as the mean over the 100-year period of lowest deep-water formation in the North Atlantic, during or right after the period of freshwater forcing. A freshwater input of 0.16 Sv allows the presence of a shallow circulation cell in the Atlantic Ocean, while a freshwater forcing of 0.35 Sv leads to an almost complete shutdown of the AMOC (Roche et al., 2014). Note that the freshwater input values needed to modify the AMOC are strongly model dependent and the important information carried by the model in the present context is the state of the AMOC rather than the freshwater input value. Contrary to ~~HS1~~ shallow overturning and off-mode streamfunctions, the Holocene streamfunction was computed using data based geostrophic velocity estimates (Talley et al., 2003).

Dissolved Pa and Th concentrations in the 2D box model are controlled by (1) production from U decay in the water column, (2) adsorption and desorption on settling particles and (3) advection by oceanic circulation. Particulate Pa and Th concentrations are controlled by (1) adsorption and desorption from the dissolved pool and (2) removal of sedimentary particles to the seafloor (Luo et al., 2010).

Modelled sedimentary meridional Pa/Th ~~meridional~~ sections generated with the different streamfunctions are shown in Fig. 2a, c, e. Different water mass ~~configurations~~ circulation intensities and geometries result in different simulated sedimentary Pa/Th (Luo et al., 2010). In the deep Atlantic, increasing circulation intensity above a specific location causes Pa/Th to decrease at that water depth because of the increased Pa export and conversely. Increasing water depth without modifying circulation intensity also causes sedimentary Pa/Th ratio to decrease in the model because of the increased residence time of Pa and resulting higher Pa export, and conversely. Finally, the sedimentary Pa/Th ratio increases along the flow path of any newly-formed water mass as ~~-~~low dissolved Pa concentrations of newly formed water masses increase by desorption of Pa from Pa-concentrated settling particles equilibrating with ambient waters (Francois, 2007). Adsorption and desorption rate constants also impact the simulated Pa/Th ratio. These constants were adjusted to reflect the opal belt in the southern ocean (Luo et al., 2010). For the Holocene, these constants were also changed to reflect preferential scavenging of Pa by biogenic opal in the northern North Atlantic (Lippold et al., 2012).

2.2.2 Limits of the models

The absence of margins in the simple 2D Pa/Th model (Luo et al., 2010) prevents it from simulating boundary scavenging, which is the lateral advection of dissolved Pa from open ocean regions characterized by high Pa concentrations to coastal regions of low Pa concentration such as in upwelling zones (Christl et al., 2010). However, as described in the results section below, we verified that our Pa/Th signal is mainly driven by oceanic circulation changes and the importance of diffusive transport is therefore likely negligible here. This simple 2D Pa/Th model therefore appears adequate for comparison with our Pa/Th data. ~~The Pa/Th model is a 2D model without parameterization of diffusive transport (Luo et al., 2010). This prevents the model from simulating boundary scavenging, which is the transfer of dissolved protactinium from open ocean regions of~~

~~high Pa concentrations to coastal regions of low Pa concentration such as in upwelling zones (Christl et al., 2010). However, as described in the results section, we verified that our Pa/Th signal is mainly driven by oceanic circulation changes and the importance of diffusive transport is therefore likely negligible here. This simple 2D Pa/Th model therefore appears adequate for comparison with our Pa/Th data.~~

The vertical resolution of the iLOVECLIM model is depth dependent, with higher resolution (10 to 100 m) in the upper water column than below 1000 m (500 to 700 m). Hence, the uncertainty in the position of the water mass transitions in the streamfunctions below 1000 m is of 500 to 700 m. However, because sedimentary Pa/Th likely reflects the ~~protactinium~~ Pa export in the bottom 1000 m of the water column (Thomas et al., 2006), the model vertical resolution is sufficient to properly simulate sedimentary Pa/Th values. ~~Moreover, benthic foraminiferal $\delta^{13}C$ measurements, which reflect the DIC of the water mass directly above the sediment interface, allows confirming or infirming the geometry information contained in measured Pa/Th values.~~ Hence, the relatively low vertical resolution of the iLOVECLIM model in the deep-ocean does not affect our conclusions.

2.3 Time slice definition

We define three interstadial and one Heinrich Stadial time slices (Fig. 3) to compare Pa/Th data measured in Atlantic cores to Pa/Th values simulated with the different streamfunctions. We focus on HS2, the preceding GI and the GIs bracketing HS4. We did not include HS4 in our study because core MD09-3257 HS4 Pa/Th data are affected by boundary scavenging (see Sect. 3.1, Burckel et al., 2015) and we therefore lack information ~~in~~ from an important location of the Atlantic Ocean.

GI-3, GI-8 and GI-10 time slices are defined as the periods of stable sedimentary Pa/Th values in core MD09-3257 associated with the NGRIP GI time intervals (Fig. 3). More specifically, we used as a reference MD09-3257 Pa/Th values bracketing the middle of NGRIP GI time intervals in the GICC05 age scale (Rasmussen et al., 2014). Contiguous Pa/Th values within 1 sigma uncertainty of the Pa/Th reference value form a plateau of stable Pa/Th values that was used to define the GI time slices. With this definition, GI time slices represent the periods of stable oceanic circulation associated with each GI. The HS2 time slice was defined in core MD09-3257 as the period of maximum sedimentary Pa/Th after the abrupt rise associated with the onset of HS2.

Sedimentary Pa/Th values associated with each time slice and core are given in Table S3. We computed uncertainties on the Pa/Th values associated with each time slice accounting for the uncertainty on individual Pa/Th measurements and uncertainties on the age model (see Supplementary Information).

Both GI-8 and -10 time slices are associated with high temperatures recorded in Greenland ice cores. The GI-3 time slice includes both the period of high Greenland temperatures associated with GI-3, and periods of low temperatures associated with GS-4 and the beginning of GS-3. Given the low Pa/Th and high $\delta^{13}C$ values in the intermediate equatorial core at that time, we consider that the GI-3 time slice mainly reflects interstadial conditions. However, because temporal resolution of the marine records is too low to clearly distinguish between GI-3 and GS-4, information about the state of the AMOC during GIs derived from this time slice should be considered with caution.

2.4 Quantification of the model-data agreement

In order to quantify the agreement between simulated and measured sedimentary Pa/Th, we compute the Euclidean distance, defined as the square root of the sum of squared differences between simulated and measured Pa/Th for each core. Minimum values indicate the best agreement between simulated and measured Pa/Th (Tables S4 and S5). Note that due to the limited number of sedimentary Pa/Th records during MIS3, we can only provide an approximate estimate of water mass boundary positions. Our equatorial transect is however ideally located to record shifts in the position of the transition between southern and northern sourced water masses.

3 Results

3.1 Sedimentary Pa/Th data

Cores MD09-3257, MD09-3256Q and SU90-03 Pa/Th measurements were centred on HS2 and HS4 (Fig. 3). No Pa/Th values were measured within HS2 in core MD09-3257 because of the presence of turbidite layers (Burckel et al., 2015). During HS4 and before HS2, the sedimentary Pa/Th ratio of core MD09-3257 rises above the production ratio of 0.093, indicating the absence of Pa export. Pa/Th variability associated with GS and GI is observed, with high Pa/Th values occurring during GS and low Pa/Th values during GI. Pa/Th variations in core MD09-3256Q are more muted (Fig. 3). The main Pa/Th variation in core MD09-3256Q occurs during HS4, when Pa/Th values rise from ~0.06 to ~0.08. This increase in MD09-3256Q Pa/Th also corresponds, within dating uncertainties, with the largest Pa/Th change from ~0.03 to ~0.05 in core SU90-03.

Before interpreting our Pa/Th records in terms of ocean circulation changes, we need to assess whether varying lithogenic or opal fluxes impacted the scavenging intensities of Pa and Th. To do so, we use the preserved opal and ^{232}Th fluxes as tracers for past opal and terrigenous fluxes respectively (Anderson et al., 2006; Lippold et al., 2012). Core MD09-3257 Pa/Th data are mainly influenced by oceanic circulation, except during the high lithogenic flux period associated with HS4 (^{232}Th flux > 12 dpm.cm^{-2}.ky^{-1}, Fig. 3a, white squares) (Burckel et al., 2015). In core MD09-3256Q, opal fluxes do not covary with the Pa/Th ratio and are very low (0.01-0.02 g.cm^{-2}.kyr^{-1}, Table S6) (Fig. S4a). In the Atlantic, the lowest opal flux value observed to influence the sedimentary Pa/Th ratio is 0.2 g.cm^{-2}.kyr^{-1} (Lippold et al., 2012). Hence, given the much lower opal fluxes recorded in core MD09-3256Q and their lack of correlation with sedimentary Pa/Th, we conclude that biogenic silica had no or very little influence on Pa/Th variability. Similarly, we find no correlation between ^{232}Th fluxes and Pa/Th values in this core (P value = 0.48, n = 22) (Fig. S5a). We can therefore safely assume that the Pa/Th variability recorded in our equatorial cores is mainly driven by changes in oceanic circulation intensity.

Core SU90-03 opal fluxes are low (< 0.1 g.cm^{-2}.kyr^{-1}, Table S6) and do not show any correlation with Pa/Th data (P value = 0.52, n = 10) (Fig. S4b). In contrast, ^{232}Th fluxes could be correlated to the Pa/Th signal (P value = 0.03, n = 16, Fig. S5b). This correlation is only driven by the highest Pa/Th value, and removing this single value results in the disappearance of the correlation (P value = 0.31, n = 15). However, we chose to keep this value as SU90-03 ^{232}Th flux is low (< ~1.5 dpm.cm^{-2}.kyr^{-1}) and its Pa/Th signal remains low (0.03-0.05) on the entire 20-50 ka period, indicating a constant significant Pa export through water mass advection. Oceanic circulation is therefore the main process explaining SU90-03 Pa/Th data.

The published Pa/Th values of other sediment cores used in this study have been shown to be mainly driven by oceanic circulation intensity (Bradtmiller et al., 2014).

3.2 C. wuellerstorfi δ13C data

C. wuellerstorfi δ^{13}C of both equatorial cores shows millennial-scale variability, with lower δ^{13}C values occurring during HS. GS and GI are also recorded in the δ^{13}C record of the intermediate core by low and high δ^{13}C values, respectively. In the deep core, the low sedimentation rate induces a low temporal resolution and a smoothing of the δ^{13}C signal that may have erased δ^{13}C decreases associated with short GS.

δ^{13}C values during the LGM are 0.24 ± 0.07 ‰ and 0.66 ± 0.06 ‰ in the deep and intermediate equatorial core, respectively (Fig. 3). Given that the late Holocene δ^{13}C measured in the equatorial cores are both close to 1.35 ‰ (see supplementary information), these LGM δ^{13}C values are much lower than what would be expected from the ~0.3‰ glacial-interglacial change in mean ocean δ^{13}C in response a reduced continental biosphere during glacial periods (Duplessy et al., 1988). The low δ^{13}C values observed during the LGM and some of the GS could thus indicate either a slowdown of the deep-water circulation, or an increased influence of southern sourced water masses at both sites during the glacial with respect to the Holocene.

3.3 Ocean circulation signals

In cores MD09-3257/GeoB3910, SU90-03 and ODP1063, GI time slices are generally characterized by lower Pa/Th and higher $\delta^{13}C$ values than those characterizing GS periods (Fig. 3). The only exception is GI-10 as this period is associated with a transition from relatively low to high Pa/Th values associated with HS4 in core SU90-03. Conversely, the HS2 time slice is associated with high Pa/Th values and low $\delta^{13}C$ values in these cores, except for core SU90-03 that exhibits Pa/Th and $\delta^{13}C$ values similar to GI time slices.

Core MD09-3256Q Pa/Th values are below 0.07 in all the studied time slices, with minor variability even between GI and HS2 time slices. Its $\delta^{13}C$ record is systematically 0.4-0.5 ‰ below that of core MD09-3257, even though the $\delta^{13}C$ difference between the two cores is reduced during HS2. Core MD09-3256Q therefore appears to be constantly bathed by a nutrient rich water mass exporting dissolved protactinium.

There is only one Pa/Th ~~data~~ value within our GI time slices in core MD02-2594 (GI-3, Fig. 3). However, two other Pa/Th values can be attributed to both GI-8 and GI-10 as they lie within these time slices considering age model uncertainties. These low MD02-2594 Pa/Th values indicate that, during GI time slices, protactinium was exported away from the intermediate-depth South Atlantic Ocean.

In addition to the above Pa/Th records, we use one Pa/Th value from core V29-172. This value lies within the GI-3 time slice and is rather low (0.04), similarly to the shallower North Atlantic core SU90-03. This supports the existence of Pa export between 1500 and 3500 m depth in the North Atlantic during GI-3.

4 Discussion

Time slice sedimentary Pa/Th data from the six selected Atlantic sediment cores are compared, when available, to the sedimentary Pa/Th pattern simulated in response to the different streamfunctions (Fig. 4-6). We focus in particular on the equatorial cores and describe their modelled and measured sedimentary Pa/Th by referring to the vertical Pa/Th gradient between 2300 and 3500 m (i.e. the water depths of the sediment cores). Indeed, vertical Pa/Th gradients are useful indicators of the vertical layout of water masses. In what follows, we will see how each vertical gradient can be interpreted.

4.1 Greenland interstadials (GI-3, GI-8 and GI-10 time slices)

4.1.1 Comparison with the Holocene simulation

A large vertical Pa/Th gradient between the two equatorial core sites is simulated by the model in the presence of a southward flowing northern-sourced deep water mass such as NADW in the Holocene simulation (Fig. 4). This is due to the fact that the sedimentary Pa/Th ratio decreases with depth within a single water mass of uniform flow rate. This effect is intensified in the case of the Holocene streamfunction, as the flow rate of NADW is not uniform but stronger between 2500-3500 m and weaker between 1300-2300 m (acquisition depths of sedimentary Pa/Th for the deep and intermediate cores respectively). Hence, Pa export at 3500 m is more intense than at 2300 m, thereby significantly increasing the vertical Pa/Th gradient between the two cores.

Interstadial Pa/Th data in the deep equatorial and North Atlantic cores are consistent with simulated Pa/Th values obtained with the Holocene streamfunction (Fig. 4b-d). However, interstadial sedimentary Pa/Th values in the equatorial core at intermediate depth are lower than predicted by the Pa/Th model forced with the Holocene streamfunction. The vertical Pa/Th gradient between our equatorial cores during interstadials is small, which is in contradiction with the large vertical Pa/Th gradient simulated with the Holocene streamfunction. Moreover, data from Southern Ocean core MD02-2594 are systematically between 0.045 and 0.050 during GI (Fig. 3), and in conflict with the high Holocene Pa/Th value (~0.09) simulated at this core site (Fig. 4).

High $\delta^{13}C$ values in the intermediate equatorial core during MIS3 interstadials suggest that northern-sourced deep waters influenced the equatorial Atlantic at 2300 m depth (Fig. 3b). However, the lower $\delta^{13}C$ values of the deep equatorial core imply that, unlike in the present-day Atlantic, nutrient-rich southern-sourced deep waters were present at 3500 m depth in the equatorial West Atlantic.
Therefore, both Pa/Th and $\delta^{13}C$ data indicate that the geometry and strength of the AMOC during the studied GI were different from those of the Holocene.

4.1.2 Comparison with the off-mode simulation

Pa/Th values simulated with the off-mode streamfunction exhibit a small vertical Pa/Th gradient between the two equatorial cores (Fig. 5). However, the sedimentary Pa/Th values measured during interstadials are much lower than the simulated values at both equatorial sites and in the North Atlantic Ocean. These low measured Pa/Th values imply a significant export of Pa by oceanic circulation and therefore exclude the possibility of an almost halted deep Atlantic circulation above 3500 m depth (Fig5, b-d).
In addition, while in the off-mode streamfunction no significant deep convection occurs in the high-latitude North Atlantic, the high $\delta^{13}C$ values of core SU90-03 and MD09-3257, and low $\delta^{13}C$ values of core MD02-2594 (< 0.5‰, Negre et al., 2010), indicate that northern sourced waters were present at ~2500 m in the North and equatorial Atlantic (Fig. 3).
Hence, it is highly unlikely that the off-mode streamfunction depicts the deep Atlantic circulation during the studied GI.

4.1.3 Comparison with the shallow overturning~~HS1~~ simulation

The shallow overturning~~HS1~~ streamfunction also induces a small vertical Pa/Th gradient between the equatorial ~~core locations~~records (Fig. 6). In contrast to the simulation obtained with the off-mode streamfunction, this small vertical Pa/Th gradient is associated with significant lateral export of Pa at the depth of both the intermediate and deep equatorial cores, as well as at the Bermuda Rise and Southern Ocean cores, in agreement with Pa/Th data (Fig. 6b-d). Such a small vertical Pa/Th gradient is simulated in the case of two water masses overlying each other and flowing in opposite directions (Fig. S6) (Lippold et al., 2012). Indeed, in the shallow overturning~~HS1~~ streamfunction, northern-sourced waters affect the depth of the intermediate equatorial core (above 2500 m). Below ~4000 m, northward flowing southern-sourced waters are active and lead to a return flow (between 2500-4000 m depth) that influences the depth of the deep equatorial core (3500 m) (Fig. 2e, f). This circulation scheme results in decreasing or invariant lateral export of Pa with depth, which in turns causes sedimentary Pa/Th to increase or to be constant with depth at the equator.
However, the agreement between simulated and measured Pa/Th in the Atlantic Ocean cores is lower (i.e. larger Euclidean distances, Table S4) with the shallow overturning~~HS1~~ streamfunction than with the Holocene streamfunction. The better model-data agreement obtained with the Holocene streamfunction is driven by the Pa/Th data of the intermediate and deep mid-latitude North Atlantic cores (SU90-03 and V29-172), as the deep convection of NADW induces low modelled Pa/Th values south of 50°N. In the shallow overturning~~HS1~~ streamfunction, the region of deep-water formation is shifted southward (Fig. 2). In the Pa/Th model, dissolved protactinium and thorium concentrations are therefore vertically homogenized between 40 and 60°N (against 60-70°N in the case of the Holocene streamfunction), preventing the presence of low sedimentary Pa/Th values north of ~40°N. A southward shift in the deep convection zone during the last glacial has been observed in earlier studies (e.g. Vidal et al., 1997), but the simulated southward shift in the present shallow overturning~~HS1~~ streamfunction could be overestimated. Assuming a more northerly position of the region of deep-water formation, the Pa/Th observed in the North Atlantic cores would agree with the shallow overturning~~HS1~~ streamfunction. Indeed, if we remove both mid-latitude North Atlantic cores from the computation of the sum of squared residuals, we find that the shallow overturning~~HS1~~ streamfunction best explains the Pa/Th data observed during GI (Table S5).

Interstadial benthic $\delta^{13}C$ values at the equator indicate the presence of (1) a northern-sourced water mass at the intermediate core site and (2) ~~of~~ a southern-sourced water mass at the deep core site (Fig. 3b). Hence, benthic $\delta^{13}C$ data support the existence of two water masses overlying each other and flowing in opposite directions as in the shallow overturning~~HS1~~ streamfunction. Moreover, the southern sourced water mass likely affected core MD02-2594 on its way towards the deep equator site as reflected by its low benthic $\delta^{13}C$ (< 0.5 ‰, Negre et al., 2010).

Based on our definition of the Interstadial time slices, we assume that the GI3 time slice reflects interstadial conditions. However, because GI3 seen in Greenland ice cores is of relatively short duration, the Pa/Th signal of the studied sediment cores might not reflect full interstadial circulation conditions. Nonetheless, we consider it unlikely that the Pa/Th of GI3 reflects stadial conditions. Indeed, core MD09-3257 sedimentary Pa/Th values observed during GI3 are similar to those recorded during the GI8 and GI10 time slices that correspond to strict interstadials (Fig. 3).

There are several studies discussing a potential link between D-O events and Atlantic circulation changes (Gottschalk et al., 2015: see Boyle, 2000 for a review), but to our knowledge, there has been no study about the geometry of the AMOC water masses during these periods. Combining the information provided by sedimentary Pa/Th and benthic foraminiferal $\delta^{13}C$ data, we reach the following conclusions concerning the Atlantic circulation below ~1300 m during the studied GI. A southward-flowing northern-sourced water mass likely circulated above ~2500 m, while southern-sourced deep water circulated northwards below ~4000 m, and southwards as a return flow between ~2500 and 4000 m depth (Fig. 2f, Fig. 7a). Moreover, our data indicate that the geometry and state of the AMOC appear similar for GI-3, -8 and -10, despite the different ice sheet volumes characterizing the periods encompassing HS2 and HS4 respectively.

4.1.4 Estimation of the AMOC intensity over the interstadial time slices

Our Holocene equatorial Pa/Th values are in reasonable agreement with previously published data from the Brazilian margin (Lippold et al., 2011) and with Pa/Th values simulated with a 2 and 3 fold increased Holocene streamfunction (Fig. S7). At present, increasing the Holocene streamfunction is indeed necessary to improve the agreement between simulated and measured equatorial Pa/Th values (Lippold et al., 2011). This increase was proposed to account for the absence of west-east difference in circulation strength in the 2D Pa/Th model, which reflects a zonally averaged circulation. Moreover, the width of the Atlantic basin is the shortest at the equator, while it is assumed constant in the model. Both these effects could cause the flow speed at the equator to be underestimated, and therefore the simulated Pa/Th ratio to be overestimated.

We performed sensitivity tests of the Pa/Th model to varying flow rates by multiplying the shallow overturning~~HS1~~ streamfunction by a factor of 1, 2 and 3. Our results indicate that factors of 1 and 2 best reproduce the sedimentary Pa/Th ratio in the Atlantic during GI time slices (Table S5).

When using the shallow overturning~~HS1~~ streamfunction, the flow of both the northern and southern sourced water masses at the equator is of 5-10 Sv. As this streamfunction amplified by a factor 1 and 2 best agrees with our interstadial Pa/Th data, we assume that the water-mass flow rates provided by these shallow overturning~~HS1~~ streamfunctions (5-20 Sv) depict well the oceanic circulation strength during the studied interstadials. The modern flow rates of NADW (northern-sourced water mass) and AABW (southern-sourced water mass) are ~27 ± 7 and ~3 Sv at 4.5°S respectively (Lux et al., 2001). We conclude that during GI-3, -8 and -10, the flow rate of the southern-sourced deep water was likely larger than present day AABW, and that the flow rate of the northern-sourced deep water may have been smaller than present-day NADW.

4.2 Heinrich Stadial 2

4.2.1 Comparison with the shallow overturning~~HS1~~ simulation

Pa/Th data from the HS2 time slice display a large vertical Pa/Th gradient between the depths of our equatorial cores (Fig. 4a, 5a, or 6a). The gradient results from the high Pa/Th value at intermediate depth, which indicates that the core was likely overlain by sluggish waters. Pa/Th data in the equatorial cores are therefore incompatible with the low vertical Pa/Th gradient simulated by the shallow overturning~~HS1~~ streamfunction (Fig. 6, Table S4).

Moreover, the decrease in benthic $\delta^{13}C$ values in both equatorial cores during HS2 ~~suggests an increased influence of southern-sourced deep waters in the deep Atlantic at both 3500 and 2300 m, which~~ is incompatible with the active northern sourced circulation cell simulated above 2500 m with the shallow overturning~~HS1~~ streamfunction (Fig. 3, b).

Hence, both circulation and ventilation proxies indicate that there was no intense northern sourced water flow between 1300 and 2300 m depth at the equator during HS2.

4.2.2 Comparison with the Holocene simulation

Large vertical Pa/Th gradients are simulated in the model when a single water mass affects both equatorial cores. Pa/Th values simulated with the Holocene streamfunction therefore best fit Pa/Th data during HS2 (Fig. 4a, Table S4). However, the very low benthic $\delta^{13}C$ values measured in both equatorial cores during HS (Fig. 3b) exclude the presence of an active northern sourced deep-water mass in the intermediate and deep equatorial Atlantic at that time.

Hence, it is unlikely that the Holocene streamfunction depicts the geometry and strength of the AMOC during HS2.

4.2.3 Comparison with the off-mode simulation

In contrast, Pa/Th values simulated with the off-mode streamfunction could reconcile the large Pa/Th vertical gradient and the low $\delta^{13}C$ of equatorial cores (Fig. 5a). In the current off-mode simulation by the iLOVECLIM model, the vertical extent of the southern-sourced water mass is not large enough to influence the equatorial core at 3500 m depth, resulting in an apparent low vertical Pa/Th gradient (Fig. 2c, d). However, the model was run for a short period of time, preventing a full response of the southern sourced deep waters to varying climatic and oceanographic conditions (Roche et al., 2014). Hence, the vertical extent of the southern sourced water mass could be larger, thereby inducing a low sedimentary Pa/Th ratio in the deepest core of the Brazilian margin. Pa/Th data from the Bermuda Rise and South Atlantic cores are consistent with simulated Pa/Th values from the off-mode streamfunction. However, the Pa/Th data from the intermediate North Atlantic core is not in agreement with the modelled Pa/Th, as there is no deep-water formation in the high latitude North Atlantic in the off-mode streamfunction.

The very low benthic $\delta^{13}C$ values measured in the deep equatorial core during HS2 ~~is~~ are consistent with the simulation using the off-mode streamfunction, which shows a strong influence of southern sourced water masses in the deep Atlantic. This is further supported by the increased ε_{Nd} in the Bermuda Rise core which indicates an increased influence of southern-sourced water masses at 4500 m in the North Atlantic Ocean during HS2 (Gutjahr and Lippold, 2011).

The off-mode simulation could therefore explain both Pa/Th and $\delta^{13}C$ values in the deep Atlantic and intermediate equatorial Atlantic, but neither this streamfunction nor the others are able to explain the Pa/Th record of the North Atlantic core at ~2500 m depth.

4.2.4 Geometry and strength of the AMOC ~~at the onset of~~during HS2

The low Pa/Th and high benthic $\delta^{13}C$ observed in core SU90-03 indicates that deep convection was still active in the high latitude North Atlantic during HS2. However, the resulting water mass was probably slow enough so that its nutrient content significantly raised on its way towards the equator either through turbulent and diffusive mixing with the underlying water mass or through the degradation of ^{12}C rich organic matter sinking from surface waters. This would explain the low $\delta^{13}C$ values measured in the intermediate equatorial core. Similarly, a long transit time of the water mass from the North Atlantic deep convection sites to the Brazilian margin could explain the high Pa/Th values measured in the intermediate equatorial core, as dissolved Pa was allowed sufficient time to equilibrate through reversible exchange with particulate matter. This progressive equilibration ~~would~~ could have led to the sedimentary Pa/Th latitudinal gradient observed at ~2500 m depth, from low sedimentary Pa/Th values in the mid-latitude North Atlantic (SU90-03) to high values in the equatorial Atlantic (MD09-3257) (Fig. 5a).

Considering that both Pa/Th and benthic $\delta^{13}C$ values suggest an increased influence of southern sourced waters at the equatorial and Bermuda Rise deep sites, the off-mode streamfunction ~~likely~~ best depicts the geometry of the AMOC during HS2 below 2500 m, i.e. southern-sourced deep waters likely ~~dominated~~ filled the deep Atlantic Ocean (Fig. 7b). The ~~direct~~ influence of the southern-sourced water mass likely extended vertically above 3500 m depth, probably at least up to 2500 m depth, as indicated by the low Pa/Th value of the deep equatorial core. However, given the discrepancy between the off-mode simulation and observed Pa/Th values in the North Atlantic intermediate core, it is difficult to assess the exact ~~position~~ latitudinal and vertical extent of the southern sourced waters ~~and their associated return flow~~. Above 2500 m, a weak water flow originating from Northern deep convection sites ~~likely~~ probably influenced the Atlantic, perhaps down to equatorial latitudes (Fig. 7b).

The geometry of the Atlantic deep water masses inferred from our sedimentary Pa/Th and benthic $\delta^{13}C$ records during HS2 is consistent with previous modelling experiments (e.g. Ganopolski and Rahmstorf, 2001) and with water mass ventilation (Elliot et al., 2002; Vidal et al., 1997; Zahn et al., 1997) and circulation intensity (Gherardi et al., 2005; McManus et al., 2004) proxies indicating that deep water circulation slowed down during Heinrich Stadials. Furthermore, our data indicate that a northern-sourced water mass was active above 2500 m during HS2, as inferred for HS1 (Gherardi et al., 2009; Roche et al., 2014) and HS2 (Lynch-Stieglitz et al., 2014; Wary et al., 2015) in previous studies. However, quantifying the intensity of the AMOC upper circulation cell during this period remains difficult since there is at present no numerical simulation in reasonably good agreement with both the circulation and ventilation proxies measured in the Atlantic.

5 Conclusions

We have shown that both the geometry and strength of the AMOC during three interstadials of the last glacial period (i.e. the GI-3, GI-8 and GI-10 intervals) was markedly different from those of the modern AMOC. Our data suggest that a northern-sourced water mass circulated above 2500 m depth with a flow rate ranging between 5 and 20 Sv, which is lower than the intensity of present-day NADW. Below 4000 m, a southern-sourced deep water mass likely flowed northward with an intensity of 5-20 Sv, which is larger than the modern AABW flow rate. Between 2500 and 4000 m depth, the southern-sourced deep water likely circulated southwards as a return flow.

Our data also show that the geometry of the AMOC likely changed ~~changed~~ at the onset of HS2 and that the deep Atlantic below 2500 m was then probably dominated by a single southern-sourced water mass that can be traced up to 35°N at 4500 m. This water mass probably ~~directly~~ affected the equatorial Atlantic between 2500 and 3500 m depth. A slow southward flowing water likely circulated between 1500 and 2500 m in the North Atlantic, but its presence at the equator remains difficult to assess.

Author contribution

P. Burckel, C. Waelbroeck, S. Pichat, J. Gherardi and J. Lippold designed the research, P. Burckel, S. L. Jaccard, and F. Thil performed the sedimentary Pa/Th measurements, S. L. Jaccard and J. Lippold performed the opal measurements, A. Govin performed the XRF measurements, Y. Luo generated the simulated Pa/Th data and D. Roche generated the streamfunctions. P. Burckel and C. Waelbroeck wrote the manuscript.

Data availability

Data related to this article are available as Supplementary Information files.

Acknowledgments

Pa/Th measurements were funded by the CNRS/INSU LEFE project ACCENT. This work is a contribution to the RETRO project, a joint European Science Foundation (ESF)/EUROMARC, funded by Research Council of Norway (RCN), France (CNRS/INSU), Germany, and the Netherlands, and to the ACCLIMATE ERC project. The research leading to these results has received funding from the European Research Council under the European Union's Seventh Framework Programme (FP7/2007-2013)/ERC grant agreement n° 339108. S.L.J. was funded by the Swiss National Foundation (grants PBEZ2-111588 and PP00P2_144811). Cores MD09-3256Q and MD09-3257 were collected on board R/V Marion Dufresne during RETRO Cruise III, supported by ESF EUROMARC project RETRO, IPEV and ANR project ANR-09-BLAN-0347. We thank the IPEV team, crew members of R/V Marion Dufresne and all scientists who participated in RETRO Cruise III. We are thankful to M. Roy-Barman for expert advices on Pa/Th measurements on LSCE MC-ICP-MS. We acknowledge C. Moreau, J.-P. Dumoulin, and the UMS ARTEMIS for AMS ^{14}C dates, and G. Isguder, L. Mauclair and F. Dewilde for invaluable technical assistance. This is LSCE contribution 5757.

~~Pa/Th measurements were funded by the CNRS/INSU LEFE project ACCENT. This work is a contribution to the RETRO project, a joint European Science Foundation (ESF)/EUROMARC, funded by Research Council of Norway (RCN), France (CNRS/INSU), Germany, and the Netherlands, and to the ACCLIMATE ERC project. The research leading to these results has received funding from the European Research Council under the European Union's Seventh Framework Programme (FP7/2007-2013)/ERC grant agreement n° 339108. Cores MD09-3256Q and MD09-3257 were collected on board R/V Marion Dufresne during RETRO Cruise III, supported by ESF EUROMARC project RETRO, IPEV and ANR project ANR-09-BLAN-0347. We thank the IPEV team, crew members of R/V Marion Dufresne and all scientists who participated in RETRO Cruise III. We are thankful to M. Roy-Barman for expert advices on Pa/Th measurements on LSCE MC-ICP-MS. We acknowledge C. Moreau, J.-P. Dumoulin, and the UMS ARTEMIS for AMS ~~^{14}C~~ dates, and G. Isguder, L. Mauclair and F. Dewilde for invaluable technical assistance. This is LSCE contribution xxxx.~~

References

Anderson, R. F., Fleisher, M. Q. and Lao, Y.: Glacial-interglacial variability in the delivery of dust to the central equatorial Pacific Ocean, Earth Planet. Sci. Lett., 242(3-4), 406–414, doi:10.1016/j.epsl.2005.11.061, 2006.

Böhm, E., Lippold, J., Gutjahr, M., Frank, M., Blaser, P., Antz, B., Fohlmeister, J., Frank, N., Andersen, M. B. and Deininger, M.: Strong and deep Atlantic meridional overturning circulation during the last glacial cycle, Nature, 517(7532), 73–76 [online] Available from: http://dx.doi.org/10.1038/nature14059, 2015.

Bourillet, J.-F., Damy, G., Dussud, L., Sultan, N., Woerther, P. and Migeon, S.: Behaviour Of A Piston Corer From Accelerometers And New Insights On Quality Of The Recovery., Proc. 6th Int. Off shore Site Investig. Geotech. Conf. Confronting New Challenges Shar. Knowledge, 11–13 Sept. 2007, London, UK. [online] Available from: http://archimer.ifremer.fr/doc/00071/18198/, 2007.

Boyle, E. a.: Is ocean thermohaline circulation linked to abrupt stadial/interstadial transitions?, Quat. Sci. Rev., 19(1-5), 255–272, doi:10.1016/S0277-3791(99)00065-7, 2000.

Bradtmiller, L. I., McManus, J. F. and Robinson, L. F.: 231Pa/230Th evidence for a weakened but persistent Atlantic meridional overturning circulation during Heinrich Stadial 1, Nat. Commun., 5, 5817, doi:10.1038/ncomms6817, 2014.

Broecker, W. S., Peteet, D. M. and Rind, D.: Does the ocean-atmosphere system have more than one stable mode of operation?, Nature, 315, 21–26, doi:10.1038/315021a0, 1985.

Burckel, P., Waelbroeck, C., Gherardi, J. M., Pichat, S., Arz, H., Lippold, J., Dokken, T. and Thil, F.: Atlantic Ocean circulation changes preceded millennial tropical South America rainfall events during the last glacial, Geophys. Res. Lett., 42(2), 411–418, doi:10.1002/2014GL062512, 2015.

Chapman, M. R., Shackleton, N. J. and Duplessy, J.-C.: Sea surface temperature variability during the last glacial–interglacial cycle: assessing the magnitude and pattern of climate change in the North Atlantic, Palaeogeogr. Palaeoclimatol. Palaeoecol., 157(1–2), 1–25, doi:http://dx.doi.org/10.1016/S0031-0182(99)00168-6, 2000.

Chase, Z., Anderson, R. F., Fleisher, M. Q. and Kubik, P. W.: The influence of particle composition and particle flux on scavenging of Th, Pa and Be in the ocean, Earth Planet. Sci. Lett., 204(1-2), 215–229, doi:10.1016/S0012-821X(02)00984-6, 2002.

Choi, M. S., Francois, R., Sims, K., Bacon, M. P., Brown-Leger, S., Fleer, a P., Ball, L., Schneider, D. and Pichat, S.: Rapid determination of ^{230}Th and ^{231}Pa in seawater by desolvated micro-nebulization Inductively Coupled Plasma magnetic sector mass spectrometry, Mar. Chem., 76(1), 99–112 [online] Available from: http://www.sciencedirect.com/science/article/pii/S0304420301000500\npapers2://publication/uuid/E489780C-06DF-45C7-ADF7-4B27109D4CBF, 2001.

Christl, M., Lippold, J., Hofmann, A., Wacker, L., Lahaye, Y. and Synal, H. A.: 231Pa/230Th: A proxy for upwelling off the coast of West Africa, Nucl. Instruments Methods Phys. Res. Sect. B Beam Interact. with Mater. Atoms, 268(7-8), 1159–1162, doi:10.1016/j.nimb.2009.10.123, 2010.

Coplen, T. B.: Normalization of oxygen and hydrogen isotope data, Chem. Geol. Isot. Geosci. Sect., 72(4), 293–297, doi:http://dx.doi.org/10.1016/0168-9622(88)90042-5, 1988.

Curry, W. B. and Oppo, D. W.: Glacial water mass geometry and the distribution of delta 13C of Sigma CO2 in the western Atlantic Ocean, Paleoceanography, 20(1), 1–12, doi:10.1029/2004PA001021, 2005.

Curry, W. B., Duplessy, J. C., Labeyrie, L. D. and Shackleton, N. J.: Changes in the distribution of δ13C of deep water ΣCO2 between the Last Glaciation and the Holocene, Paleoceanography, 3(3), 317–341, doi:10.1029/PA003i003p00317, 1988.

Duplessy, J. C., Shackleton, N. J., Fairbanks, R. G., Labeyrie, L., Oppo, D. and Kallel, N.: Deepwater source variations during the last climatic cycle and their impact on the global deepwater circulation, Paleoceanography, 3(3), 343–360, doi:10.1029/PA003i003p00343, 1988.

Duplessy, J.-C., Shackleton, N. J., Matthews, R. K., Prell, W., Ruddiman, W. F., Caralp, M. and Hendy, C. H.: 13C Record of benthic foraminifera in the last interglacial ocean: Implications for the carbon cycle and the global deep water circulation, Quat. Res., 21(2), 225–243, doi:10.1016/0033-5894(84)90099-1, 1984.

Elliot, M., Labeyrie, L. and Duplessy, J. C.: Changes in North Atlantic deep-water formation associated with the Dansgaard - Oeschger temperature oscillations (60-10 ka), Quat. Sci. Rev., 21(10), 1153–1165, doi:10.1016/S0277-3791(01)00137-8, 2002.

Francois, R.: Paleoflux and Paleocirculation from Sediment 230Th and 231Pa/230Th, in Proxies in Late Cenozoic Paleoceanography, vol. 1, pp. 681–716, Elsevier., 2007.

Ganopolski, A. and Rahmstorf, S.: Rapid changes of glacial climate simulated in a coupled climate model., Nature, 409(6817), 153–158, doi:10.1038/35051500, 2001.

Gherardi, J. M., Labeyrie, L., McManus, J. F., Francois, R., Skinner, L. C. and Cortijo, E.: Evidence from the Northeastern Atlantic basin for variability in the rate of the meridional overturning circulation through the last deglaciation, Earth Planet. Sci. Lett., 240(3-4), 710–723, doi:10.1016/j.epsl.2005.09.061, 2005.

Gherardi, J. -M., Labeyrie, L., Nave, S., Francois, R., McManus, J. F. and Cortijo, E.: Glacial-interglacial circulation changes inferred from 231Pa/230Th sedimentary record in the North Atlantic region, Paleoceanography, 24(2), 1–14, doi:10.1029/2008PA001696, 2009.

Gottschalk, J., Skinner, L. C., Misra, S., Waelbroeck, C., Menviel, L. and Timmermann, A.: Abrupt changes in the southern extent of North Atlantic Deep Water during Dansgaard-Oeschger events, Nat. Geosci, 8(12), 950–954 [online] Available from: http://dx.doi.org/10.1038/ngeo2558, 2015.

Guihou, A., Pichat, S., Nave, S., Govin, A., Labeyrie, L., Michel, E. and Waelbroeck, C.: Late slowdown of the Atlantic Meridional Overturning Circulation during the Last Glacial Inception: New constraints from sedimentary (231Pa/230Th), Earth Planet. Sci. Lett., 289(3-4), 520–529, doi:10.1016/j.epsl.2009.11.045, 2010.

Guihou, A., Pichat, S., Govin, A., Nave, S., Michel, E., Duplessy, J. C., Telouk, P. and Labeyrie, L.: Enhanced Atlantic Meridional Overturning Circulation supports the Last Glacial Inception, Quat. Sci. Rev., 30(13-14), 1576–1582, doi:10.1016/j.quascirev.2011.03.017, 2011.

Gutjahr, M. and Lippold, J.: Early arrival of Southern Source Water in the deep North Atlantic prior to Heinrich event 2, Paleoceanography, 26(2), 1–9, doi:10.1029/2011PA002114, 2011.

Hall, I. R., Moran, S. B., Zahn, R., Knutz, P. C., Shen, C. C. and Edwards, R. L.: Accelerated drawdown of meridional overturning in the late-glacial Atlantic triggered by transient pre-H event freshwater perturbation, Geophys. Res. Lett., 33(16), 1–5, doi:10.1029/2006GL026239, 2006.

Heinrich, H.: Origin and consequences of cyclic ice rafting in the Northeast Atlantic Ocean during the past 130,000 years, Quat. Res., 29(2), 142–152, doi:10.1016/0033-5894(88)90057-9, 1988.

Henry, L. G., McManus, J. F., Curry, W. B., Roberts, N. L., Piotrowski, A. M. and Keigwin, L. D.: North Atlantic ocean circulation and abrupt climate change during the last glaciation, Science (80-.)., 353(6298), 470–474, doi:10.1126/science.aaf5529, 2016.

Jaeschke, A., Rühlemann, C., Arz, H., Heil, G. and Lohmann, G.: Coupling of millennial-scale changes in sea surface temperature and precipitation off northeastern Brazil with high-latitude climate shifts during the last glacial period, Paleoceanography, 22(4), 1–10, doi:10.1029/2006PA001391, 2007.

Johnsen, S. J., Clausen, H. B., Dansgaard, W., Fuhrer, K., Gundestrup, N., Hammer, C. U., Iversen, P., Jouzel, J., Stauffer, B. and steffensen, J. P.: Irregular glacial interstadials recorded in a new Greenland ice core, Nature, 359(6393), 311–313 [online] Available from: http://dx.doi.org/10.1038/359311a0, 1992.

Jonkers, L., Zahn, R., Thomas, A., Henderson, G., Abouchami, W., Francois, R., Masque, P., Hall, I. R. and Bickert, T.: Deep circulation changes in the central South Atlantic during the past 145 kyrs reflected in a combined Pa-231/Th-230, Neodymium isotope and benthic delta C-13 record, EARTH Planet. Sci. Lett., 419, 14–21, doi:10.1016/j.epsl.2015.03.004, 2015.

Kindler, P., Guillevic, M., Baumgartner, M., Schwander, J., Landais, A. and Leuenberger, M.: Temperature reconstruction from 10 to 120 kyr b2k from the NGRIP ice core, Clim. Past, 10(2), 887–902, doi:10.5194/cp-10-887-2014, 2014.

Lambeck, K. and Chappell, J.: Sea level change through the last glacial cycle., Science, 292(5517), 679–686, doi:10.1126/science.1059549, 2001.

Lippold, J., Gherardi, J. M. and Luo, Y.: Testing the 231Pa/230Th paleocirculation proxy: A data versus 2D model comparison, Geophys. Res. Lett., 38(20), 1–7, doi:10.1029/2011GL049282, 2011.

Lippold, J., Luo, Y., Francois, R., Allen, S. E., Gherardi, J., Pichat, S., Hickey, B. and Schulz, H.: Strength and geometry of the glacial Atlantic Meridional Overturning Circulation, Nat. Geosci., 5(11), 813–816, doi:10.1038/ngeo1608, 2012.

Lippold, J., Gutjahr, M., Blaser, P., Christner, E., Ferreria, M. L. de C., Mulitza, S., Christl, M., Wombacher, F., Boehm, E., Antz, B., Cartapanis, O., Vogel, H. and Jaccard, S. L.: Deep water provenance and dynamics of the (de)glacial Atlantic meridional overturning circulation, EARTH Planet. Sci. Lett., 445, 68–78, doi:10.1016/j.epsl.2016.04.013, 2016.

Luo, Y., Francois, R. and Allen, S.: Sediment 231Pa/230Th as a recorder of the rate of the Atlantic meridional overturning circulation: insights from a 2-D model, Ocean Sci., 6(3), 381–400, doi:10.5194/os-6-381-2010, 2010.

Lux, M., Mercier, H. and Arhan, M.: Interhemispheric exchanges of mass and heat in the Atlantic Ocean in January–March 1993, Deep Sea Res. Part I Oceanogr. Res. Pap., 48(3), 605–638, doi:http://dx.doi.org/10.1016/S0967-0637(00)00033-9, 2001.

Lynch-Stieglitz, J., Stocker, T. F., Broecker, W. S. and Fairbanks, R. G.: The influence of air-sea exchange on the isotopic composition of oceanic carbon: Observations and modeling, Global Biogeochem. Cycles, 9(4), 653–665, doi:10.1029/95GB02574, 1995.

Lynch-Stieglitz, J., Schmidt, M. W., Gene Henry, L., Curry, W. B., Skinner, L. C., Mulitza, S., Zhang, R. and Chang, P.: Muted change in Atlantic overturning circulation over some glacial-aged Heinrich events, Nat. Geosci., 7(2), 1–7, doi:10.1038/ngeo2045, 2014.

McManus, J. F., Francois, R., Gherardi, J.-M., Keigwin, L. D. and Brown-Leger, S.: Collapse and rapid resumption of Atlantic meridional circulation linked to deglacial climate changes., Nature, 428(6985), 834–837, doi:10.1038/nature02494, 2004.

Negre, C., Zahn, R., Thomas, A. L., Masqué, P., Henderson, G. M., Martínez-Méndez, G., Hall, I. R. and Mas, J. L.: Reversed flow of Atlantic deep water during the Last Glacial Maximum., Nature, 468(7320), 84–88, doi:10.1038/nature09508, 2010.

Rasmussen, S. O., Bigler, M., Blockley, S. P., Blunier, T., Buchardt, S. L., Clausen, H. B., Cvijanovic, I., Dahl-Jensen, D., Johnsen, S. J., Fischer, H., Gkinis, V., Guillevic, M., Hoek, W. Z., Lowe, J. J., Pedro, J. B., Popp, T., Seierstad, I. K., Steffensen, J. P., Svensson, A. M., Vallelonga, P., Vinther, B. M., Walker, M. J. C., Wheatley, J. J. and Winstrup, M.: A stratigraphic framework for abrupt climatic changes during the Last Glacial period based on three synchronized Greenland ice-core records: refining and extending the INTIMATE event stratigraphy, Quat. Sci. Rev., 106, 14–28, doi:http://dx.doi.org/10.1016/j.quascirev.2014.09.007, 2014.

Reimer, P. J., Bard, E., Bayliss, A., Beck, J. W., Blackwell, P. G., Ramsey, C. B., Buck, C. E., Cheng, H., Edwards, R. L., Friedrich, M., Grootes, P. M., Guilderson, T. P., Haflidason, H., Hajdas, I., Hatte, C., Heaton, T. J., Hoffmann, D. L., Hogg, A. G., Hughen, K. A., Kaiser, K. F., Kromer, B., Manning, S. W., Niu, M., Reimer, R. W., Richards, D. A., Scott, E. M., Southon, J. R., Staff, R. A., Turney, C. S. M. and van der Plicht, J.: IntCal13 and Marine13 Radiocarbon Age Calibration Curves 0–50,000 years Cal BP, Radiocarbon, 55(4), 1869–1887 [online] Available from: http://apps.webofknowledge.com.biblioplanets.gate.inist.fr/full_record.do?product=UA&search_mode=GeneralSearch&qid=12&SID=R2qElS8CFcTUu7uanDW&page=1&doc=2 (Accessed 1 July 2015), 2013.

Rhein, M., Stramma, L. and Send, U.: The Atlantic Deep Western Boundary Current : Water masses and transports near the equator, , 100, 2441–2457, 1995.

Roche, D. M., Dokken, T. M., Goosse, H., Renssen, H. and Weber, S. L.: Climate of the Last Glacial Maximum: sensitivity studies and model-data comparison with the LOVECLIM coupled model, Clim. Past, 3(2), 205–224, doi:10.5194/cp-3-205-2007, 2007.

Roche, D. M., Wiersma, A. P. and Renssen, H.: A systematic study of the impact of freshwater pulses with respect to different geographical locations., Clim. Dyn., 34(7/8), 997–1013 [online] Available from: 10.1007/s00382-009-0578-8, 2010.

Roche, D. M., Paillard, D., Caley, T. and Waelbroeck, C.: LGM hosing approach to Heinrich Event 1: results and perspectives from data–model integration using water isotopes, Quat. Sci. Rev., 106, 247–261, doi:10.1016/j.quascirev.2014.07.020, 2014.

Rohling, E. and Cooke, S.: Stable oxygen and carbon isotopes in foraminiferal carbonate shells, Mod. foraminifera, c, 239–258 [online] Available from: http://www.springerlink.com/index/R519428618723716.pdf, 2003.

Schlitzer, R., Electronic Atlas of WOCE Hydrographic and Tracer Data Now Available, Eos Trans. AGU, 81(5), 45, 2000

Schlitzer, R., Ocean Data View, http://odv.awi.de, 2015

Schott, F. a.: The zonal currents and transports at 35°W in the tropical Atlantic, Geophys. Res. Lett., 30(7), 35–38, doi:10.1029/2002GL016849, 2003.

Skinner, L. C. and McCave, I. N.: Analysis and modelling of gravity- and piston coring based on soil mechanics, Mar. Geol., 199(1–2), 181–204, doi:http://dx.doi.org/10.1016/S0025-3227(03)00127-0, 2003.

Skinner, L. C., Shackleton, N. J. and Elderfield, H.: Millennial-scale variability of deep-water temperature and δ18Odw indicating deep-water source variations in the Northeast Atlantic, 0-34 cal. ka BP, Geochemistry, Geophys. Geosystems, 4(12), doi:10.1029/2003GC000585, 2003.

Talley, L. D., Reid, J. L. and Robbins, P. E.: Data-based meridional overturning streamfunctions for the global ocean, J. Clim., 16(19), 3213–3226, doi:10.1175/1520-0442(2003)016<3213:DMOSFT>2.0.CO;2, 2003.

Thomas, A. L., Henderson, G. M. and Robinson, L. F.: Interpretation of the 231Pa/230Th paleocirculation proxy: New water-column measurements from the southwest Indian Ocean, Earth Planet. Sci. Lett., 241(3-4), 493–504, doi:10.1016/j.epsl.2005.11.031, 2006.

Vidal, L., Labeyrie, L., Cortijo, E., Arnold, M., Duplessy, J.-C., Michel, E., Becqué, S. and van Weering, T. C. E.: Evidence for changes in the North Atlantic Deep Water linked to meltwater surges during the Heinrich events, Earth Planet. Sci. Lett., 146(1-2), 13–27, doi:10.1016/S0012-821X(96)00192-6, 1997.

Wary, M., Eynaud, F., Sabine, M., Zaragosi, S., Rossignol, L., Malaizé, B., Palis, E., Zumaque, J., Caulle, C., Penaud, A., Michel, E. and Charlier, K.: Stratification of surface waters during the last glacial millennial climatic events: a key factor in subsurface and deep-water mass dynamics, Clim. Past, 11(11), 1507–1525, doi:10.5194/cp-11-1507-2015, 2015.

Woerther, P. and Bourillet, J. F.: Exploitation des mesures faites avec les accéléromètres sur le carottier CAPYPSO -Mission SEDICAR4-ALIENOR., Ifremer, Brest, pp. 47 & 4 annexes, 2005.

Yu, E.-F., Francois, R. and Bacon, M. P.: Similar rates of modern and last-glacial ocean thermohaline circulation inferred from radiochemical data, Nature, 379(6567), 689–694, doi:10.1038/379689a0, 1996.

Zahn, R., Winn, K. and Sarnthein, M.: Benthic foraminiferal δ13C and accumulation rates of organic carbon: Uvigerina Peregrina group and Cibicidoides Wuellerstorfi, Paleoceanography, 1(1), 27–42, doi:10.1029/PA001i001p00027, 1986.

Zahn, R., Schönfeld, J., Kudrass, H.-R., Park, M.-H., Erlenkeuser, H. and Grootes, P.: Thermohaline instability in the North Atlantic during meltwater events: Stable isotope and ice-rafted detritus records from Core SO75-26KL, Portuguese Margin, Paleoceanography, 12(5), 696–710, doi:10.1029/97PA00581, 1997.

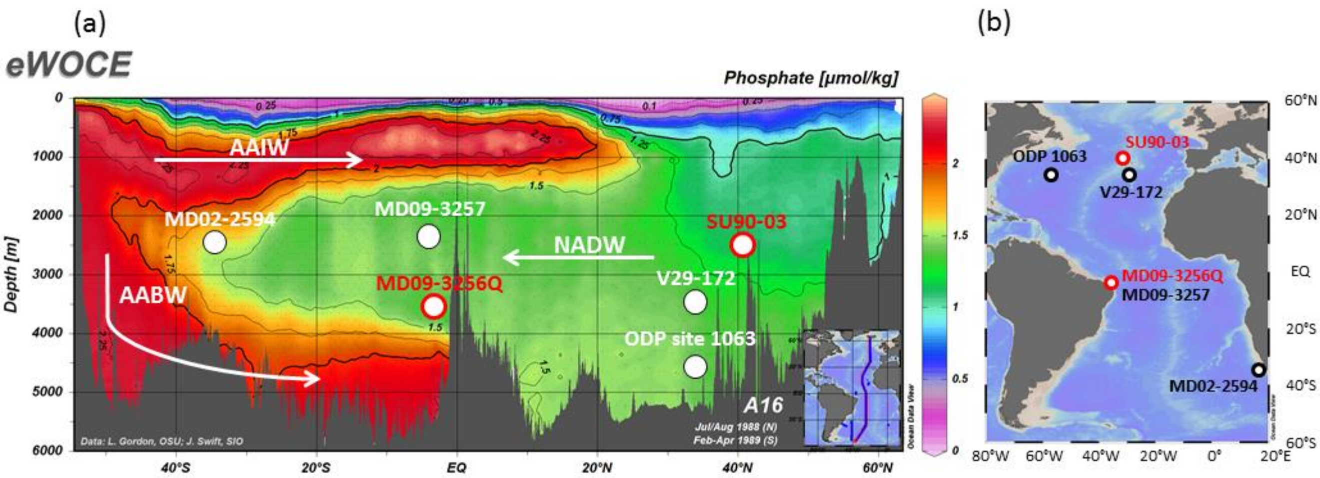

Figure 1: (a) Phosphate section (Schlitzer, 2000) and (b) map of the Atlantic Ocean ~~(Schlitzer, 2000)~~ showing the location of the studied sediment cores (see Sect. 2.1 or Table S1 for detailed locations). Cores for which we provide new Pa/Th or $\delta^{13}C$ data are circled in red. Phosphate content follows the structure of the present day AMOC. White arrows indicate the approximate flow directions of the Antarctic Intermediate Water (AAIW), Antarctic Bottom Water (AABW) and North Atlantic Deep Water (NADW).

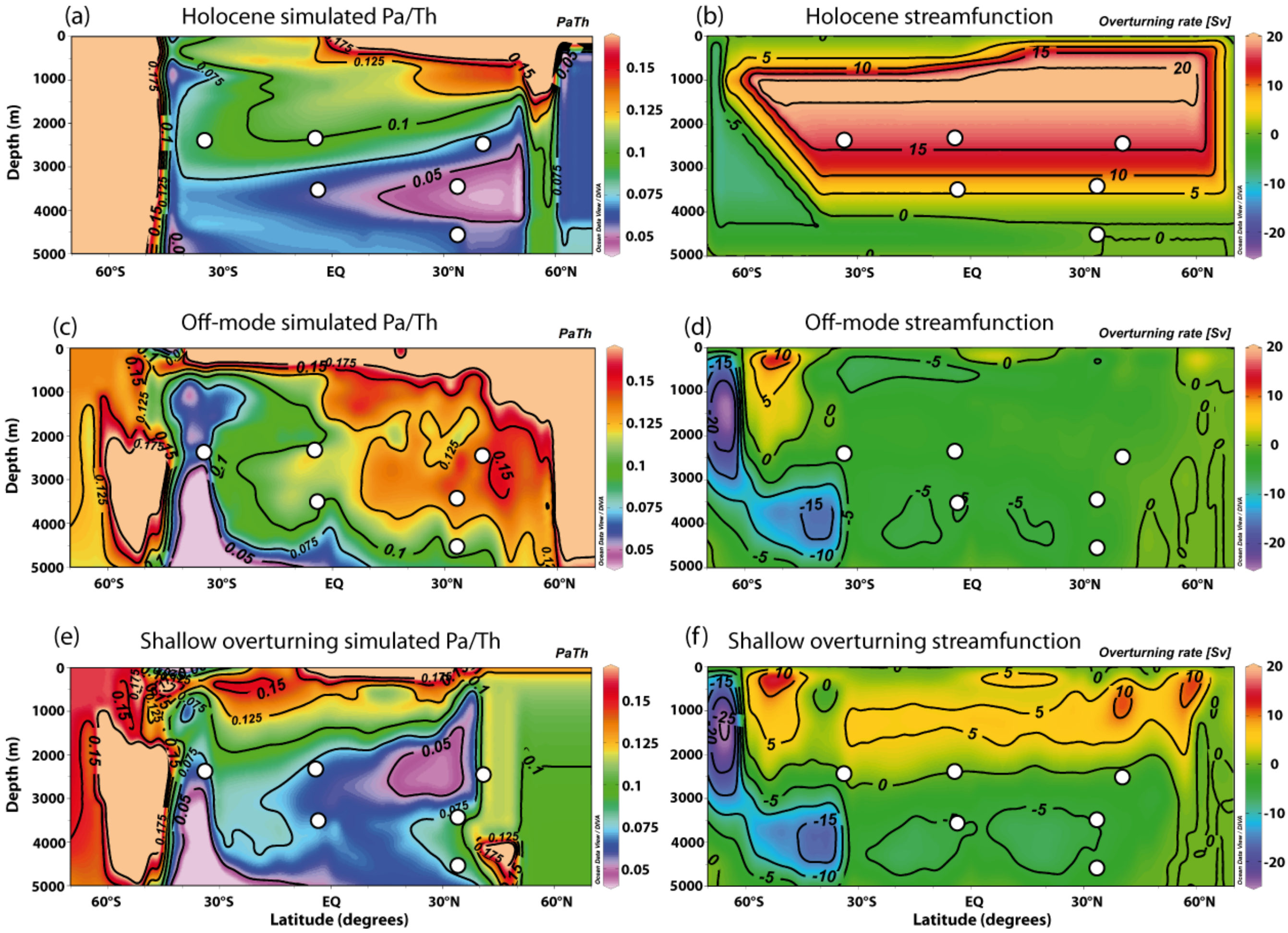

Figure 2: Simulated sedimentary Pa/Th values (left) in response to different streamfunctions (right): (a, b) Holocene, (c, d) Off-mode, (e, f) shallow overturning~~HS1~~. White dots indicate the position of the studied sediment cores (see Fig. 1). Data gridding was achieved using the Ocean Data View software (Schlitzer, 2015).

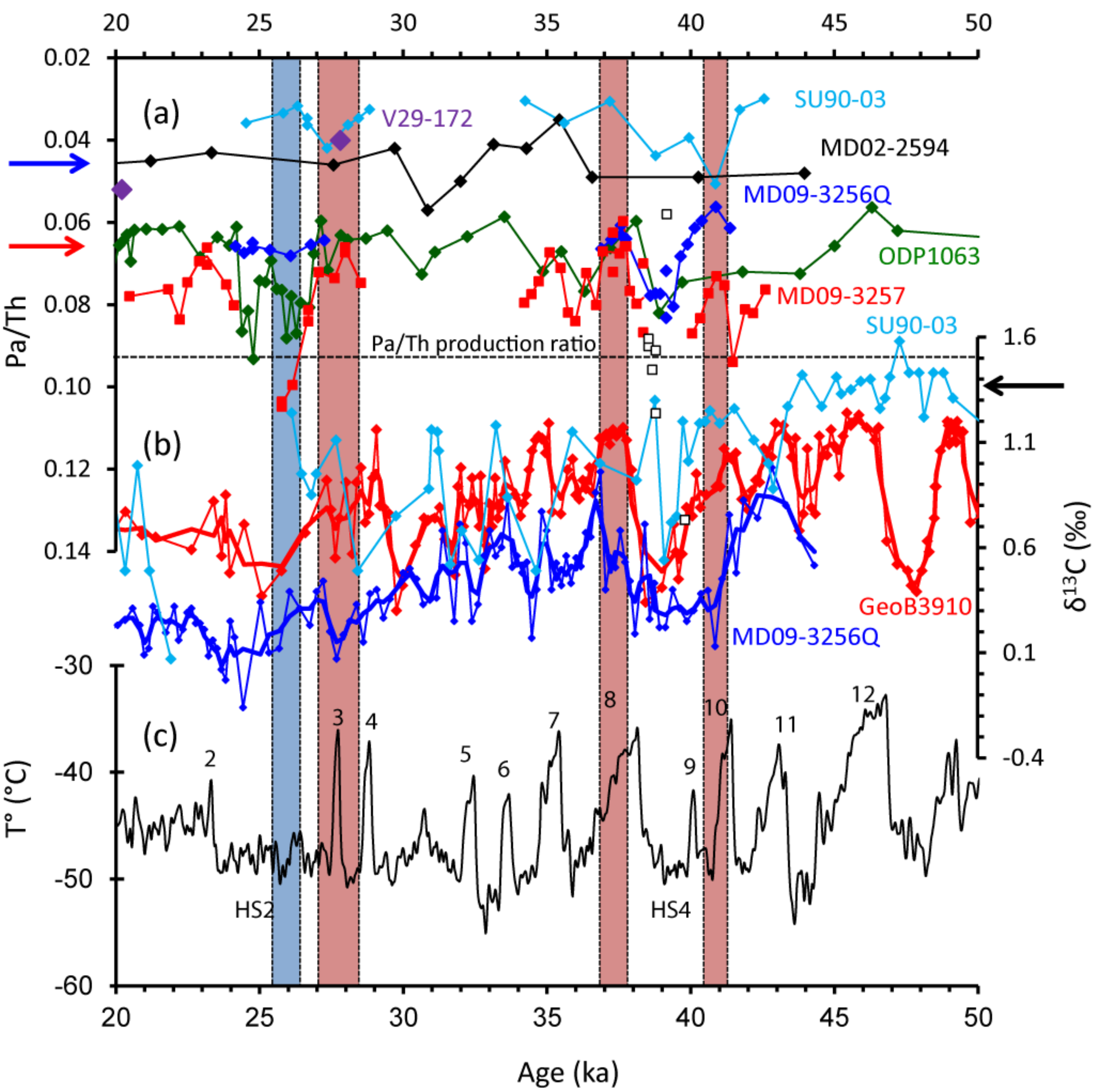

Figure 3: Comparison between sedimentary Pa/Th and benthic $\delta^{13}C$ data from the Brazilian margin, Bermuda Rise, mid-latitude North and South Atlantic Ocean and Greenland temperatures. (a) MD09-3256Q (this study), SU90-03 (this study), MD09-3257 (Burckel et al., 2015), ODP1063 (Böhm et al., 2015), MD02-2594 (Negre et al., 2010) and V29-172 (Bradtmiller et al., 2014) Pa/Th (b) MD09-3256Q (this study), SU90-03 (Chapman et al., 2000) and GeoB3910 (Burckel et al., 2015) *Cibicides wuellerstorfi* $\delta^{13}C$ and (c) NGRIP temperature record on the GICC05 timescale (Kindler et al., 2014). In (a) lines pass through average Pa/Th values in case of replicates, while diamonds and squares (MD09-3257) correspond to individual Pa/Th measurements~~In (a) the average Pa/Th for each core is represented by the lines and individual measurements by diamonds or squares (MD09-3257)~~. V29-172 Pa/Th values are represented by two purple diamonds. White squares indicate Pa/Th values not considered in core MD09-3257, as they might not be influenced by oceanic circulation only (Burckel et al., 2015). The red and blue arrows indicate the Late Holocene Pa/Th values in cores MD09-3257 (0.065 ± 0.004, Burckel et al., 2015) and MD09-3256Q (0.043±0.002), respectively. Error bars on Pa/Th measurements are given in Fig. S1 and Table S7 and S8. In (b) thick lines are 3-point running averages of the *Cibicides w.* $\delta^{13}C$ records, the black arrow indicates present day NADW $\delta^{13}C$ value (~1.36 ‰, supplementary information). $\delta^{13}C$ values are given in Table S9. In (c) numbers indicate the GI. Red vertical bands represent the GI-3, GI-8 and GI-10 time slices and the blue vertical band the HS2 time slice.

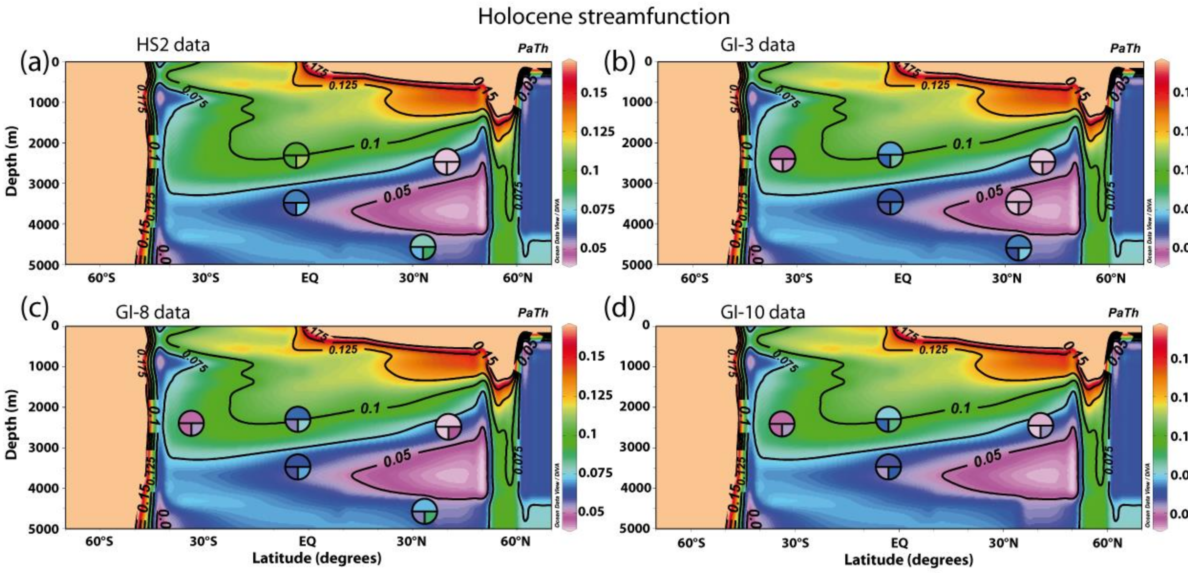

Figure 4: Comparison of the Pa/Th data (circles) for each of the time slices to the simulated Pa/Th values using the Holocene streamfunction. (a) HS2, (b) GI-3, (c) GI-8 and (d) GI-10 Pa/Th data. The upper half of the circles represents the Pa/Th mean value, the lower left quarter, the Pa/Th mean value – 1 sigma, and the lower right quarter, the Pa/Th mean value + 1 sigma. Data gridding was achieved using the Ocean Data View software (Schlitzer, 2015).

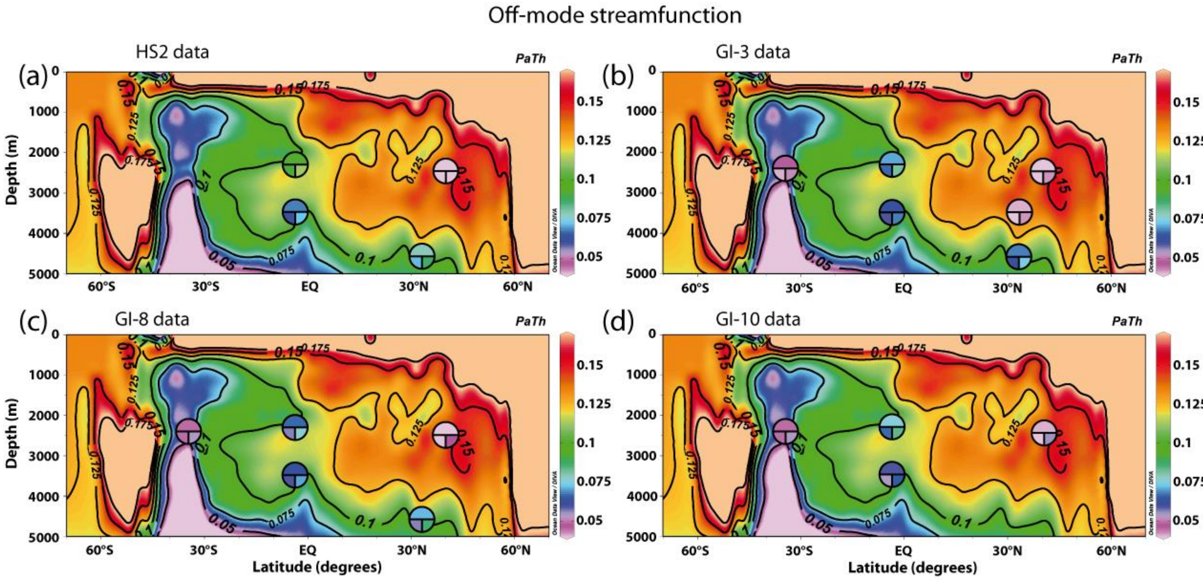

Figure 5: Comparison of the Pa/Th data for each of the time slices to the simulated Pa/Th values using the off-mode streamfunction. Time slices are (a) HS2, (b) GI-3, (c) GI-8 and (d) GI-10 Pa/Th data; symbols as in Fig. 4.

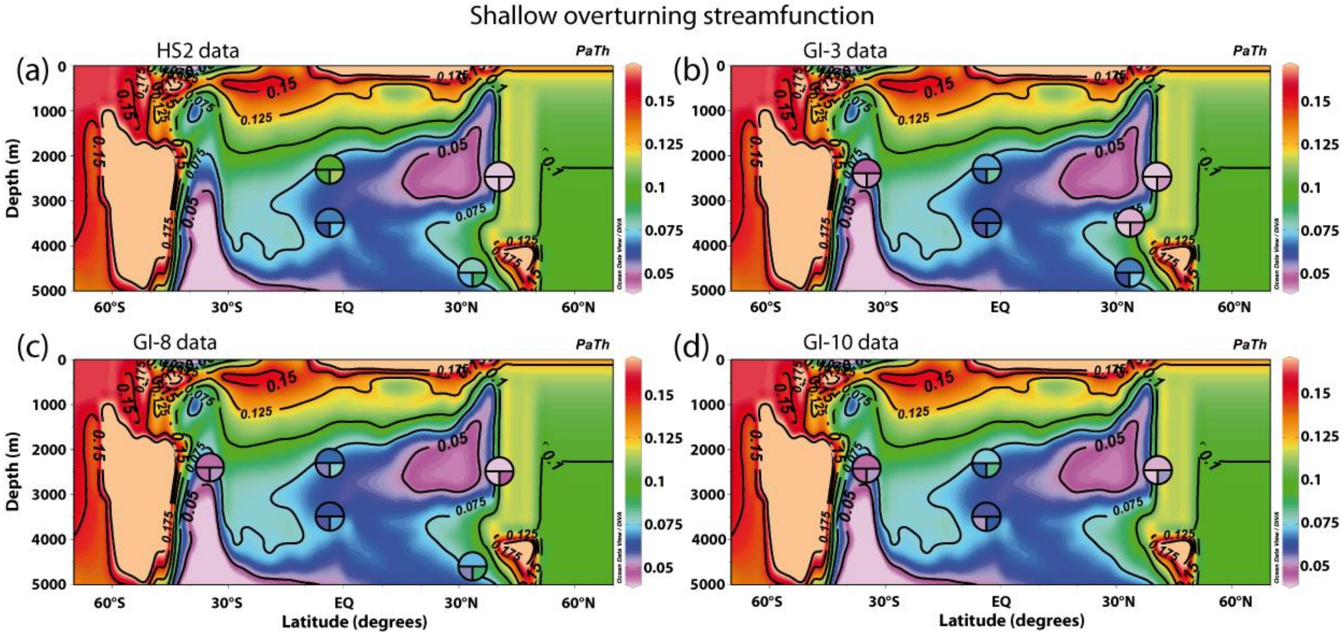

Figure 6: Comparison of the Pa/Th data for each of the time slices to the simulated Pa/Th values using the <u>shallow overturning</u>~~HS1~~ streamfunction. Time slices are (a) HS2, (b) GI-3, (c) GI-8 and (d) GI-10 Pa/Th data; symbols as in Fig. 4.

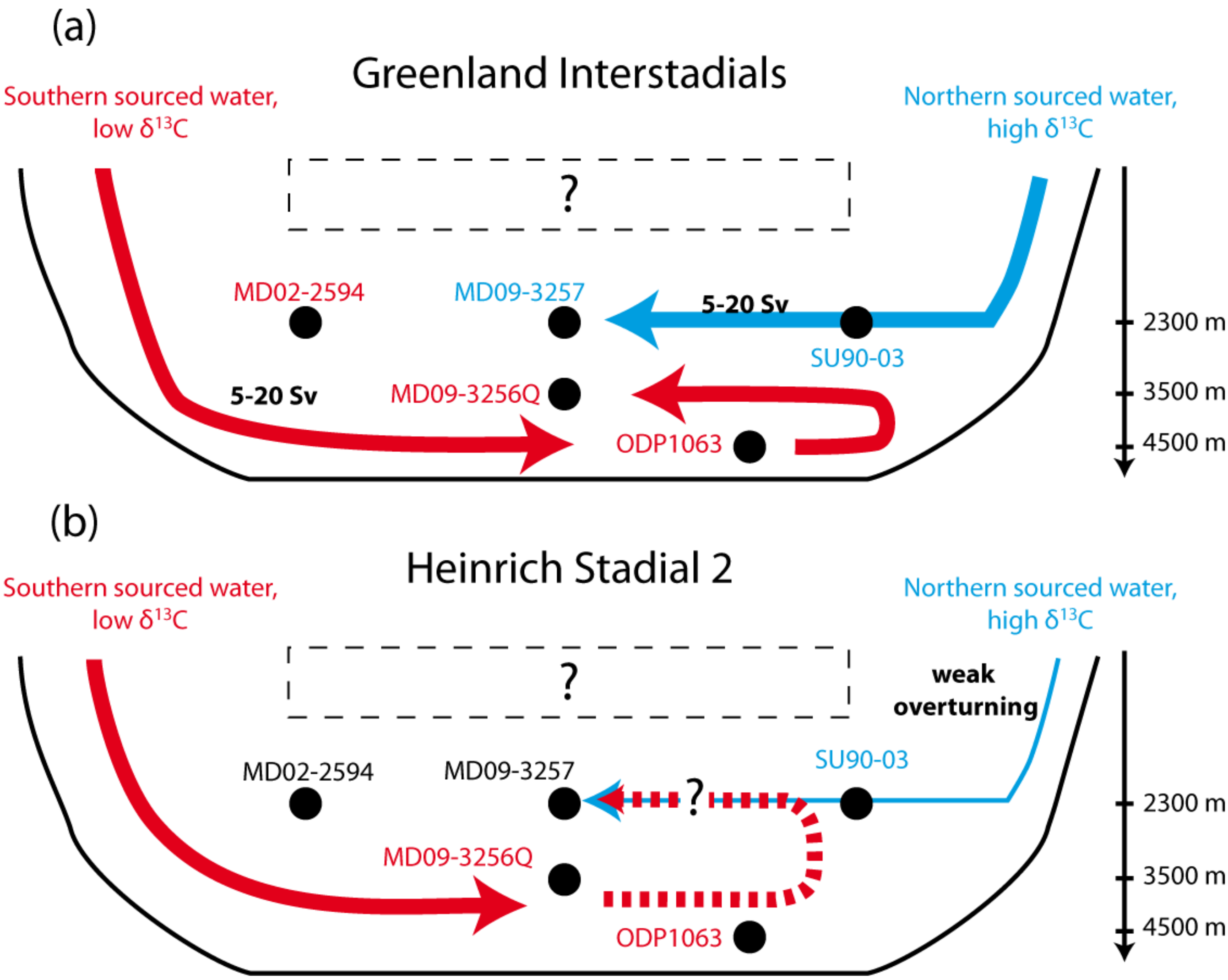

Figure 7: Sketch of the possible states of the AMOC during (a) Greenland interstadials and (b) Heinrich Stadial 2. Red and blue arrows depict the southern and northern sourced water mass, respectively. The arrows' thickness reflects the overturning rate. Core names are coloured depending on which water mass influences them. In (b), cores MD09-3257 and MD02-2594 <u>names</u> are ~~written~~ in black as ~~it is difficult to assess which water mass bathes the equator at 2300 m depth and as~~ we have no direct evidence of which

water mass influences the South Atlantic Ocean during HS2. The exact position of the northward flowing ~~southern~~ southern-sourced water mass and its possible return flow (dashed red line) is also unknown ~~in (b)~~.

S1. Holocene *C. wuellerstorfi* $\delta^{13}C$ and sedimentary Pa/Th

At present, NADW extends from 1200 to 4000 m depth in the equatorial Atlantic (Schott, 2003). In Fig. 3, the modern $\delta^{13}C$ value of NADW is set to 1.36 ± 0.09 ‰, which is the mean of the $\delta^{13}C$ values in benthic foraminifer *C. wuellerstorfi* over the Late Holocene at ~3500 and 2300 m depth on the Brazilian margin. Late Holocene $\delta^{13}C$ values are computed as the mean $\delta^{13}C$ value over the time interval 0-4 ka (Table S9). This yields Late Holocene $\delta^{13}C$ values of 1.30 ± 0.08 ‰ (n = 8) in core MD09-3256Q and 1.43 ± 0.01 ‰ (n = 2) in core MD09-3257.
Modern sedimentary Pa/Th values in Fig. 3 are based on Late Holocene sedimentary Pa/Th measurements in both equatorial cores. The Late Holocene Pa/Th value is of 0.065 ± 0.04 (1 σ) in core MD09-3257 (Burckel et al., 2015) and of 0.043 ± 0.02 (1 σ) in core MD09-3256Q (Table S7). These Pa/Th values are computed using a $^{238}U/^{232}Th$ lithogenic correction of 0.5 ± 0.1.

S2. Pa/Th uncertainties related to dating uncertainties

The Pa/Th record of core MD09-3257 is used as reference for the definition of the time slices associated with HS2 and Greenland Interstadials. Hence, Pa/Th values associated with the different time slices in core MD09-3257 are independent from the age model. For all other cores, dating uncertainties account for Pa/Th uncertainties associated with each time slice.~~Hence, Pa/Th values associated with each time slice on core MD09-3257 are invariant, despite dating uncertainties.~~ Studied sediment cores were chosen for their well-defined age model, with uncertainties small enough for their Pa/Th record to be used with confidence. We define the Pa/Th uncertainty associated with each time slice as the maximum between the Pa/Th uncertainty induced by age model uncertainties and induced by averaging Pa/Th values with their own individual uncertainties. At least one Pa/Th value has to be within a specific time slice (considering one sigma uncertainties on the age) for the core Pa/Th data to be used within this time slice.
For core ODP 1063, we considered a 500 y dating uncertainty on the 20-50 ka period (Böhm et al., 2015).
Pa/Th values and uncertainties calculated as detailed in this section are given in Table S3.

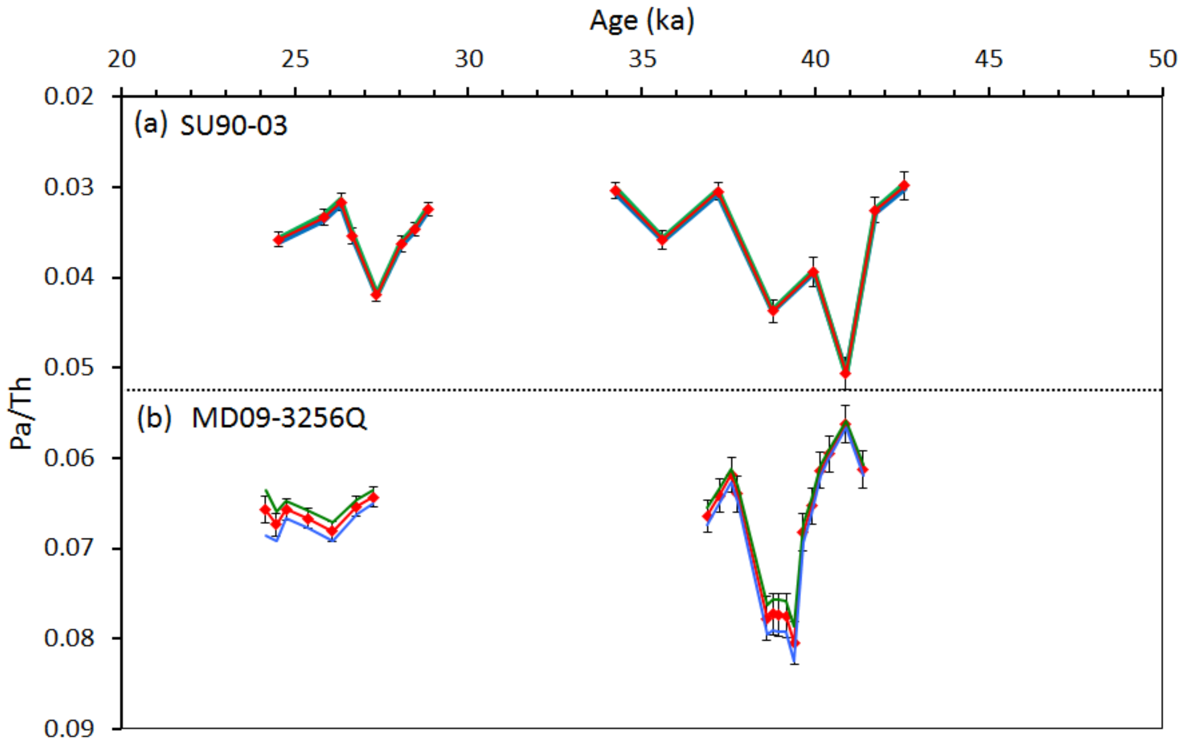

Figure S1: Pa/Th in cores SU90-03 (a) and MD09-3256Q (b) as a function of time calculated with different lithogenic ($^{238}U/^{232}Th$) (R) values used to correct for detrital material contribution (Francois, 2007). Red curve, R=0.5 (correction used in Fig. 3), green curve R=0.4, and blue curve R=0.6. Error bars are 1 SE and do not account for the error on R.

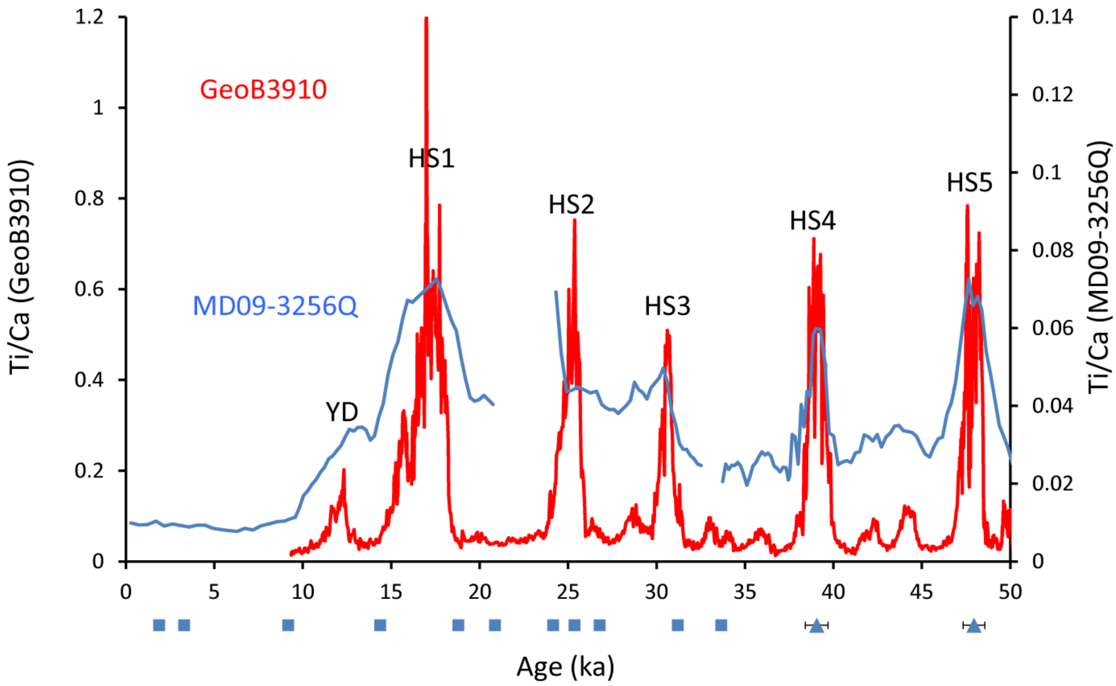

Figure S2: Core MD09-3256Q age model. Blue squares indicate the position of ^{14}C dates in core MD09-3256Q. Blue triangles indicate tie points between core GeoB3910 (red line) and MD09-3256Q (blue line) Ti/Ca records. YD and HS1-HS5 are marked by Ti/Ca peaks caused by increased precipitation and runoff in North-East Brazil during the Younger Dryas and Heinrich Stadials 1-5 (Burckel et al., 2015). Discontinuities in the Ti/Ca record of core MD09-3256Q correspond to the position of turbidite layers. Error bars are 1 sigma and include the uncertainty on correlation for the tie points.

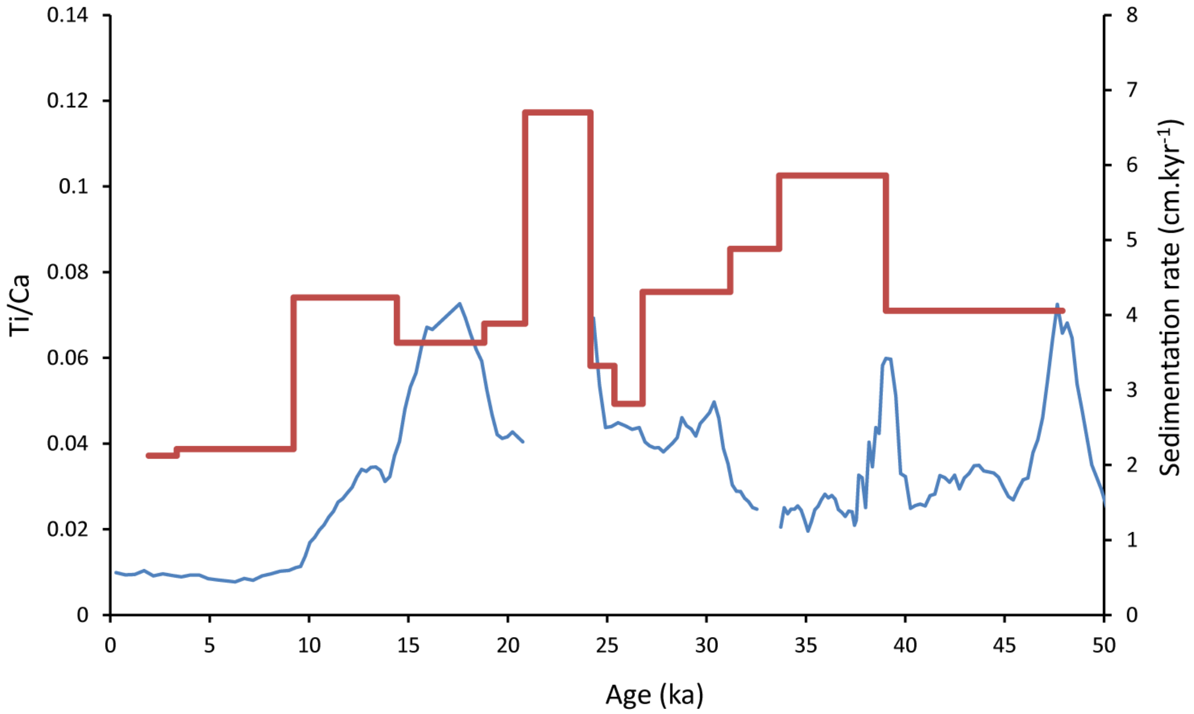

Figure S3: Core MD09-3256Q Ti/Ca record (blue curve) and sedimentation rate (red curve).

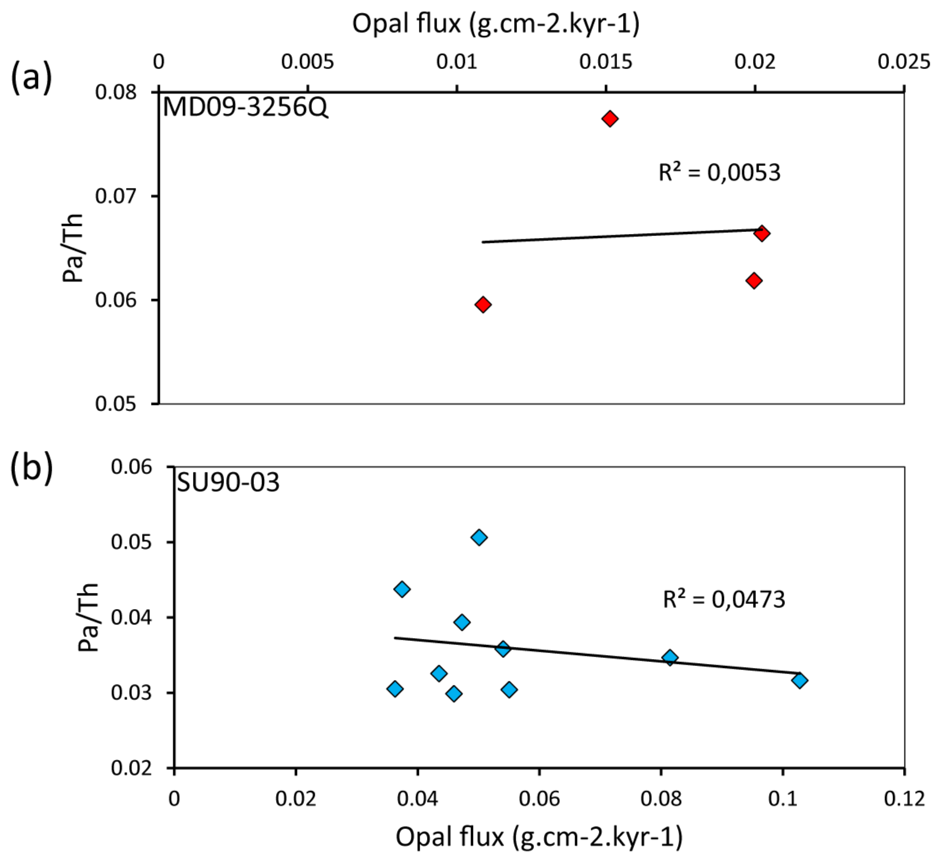

Figure S4: Assessment of the opal influence on the Pa/Th records. Sedimentary Pa/Th as a function of opal flux in core MD09-3256Q (a) and in core SU90-03 (b). ~~Assessment of the opal influence on the Pa/Th records. (a) Sedimentary Pa/Th (red) and opal flux (black) as a function of depth in core MD09-3256Q, (b) Opal flux as a function of Pa/Th in core SU90-03. In (a), error bars are 1 sigma.~~

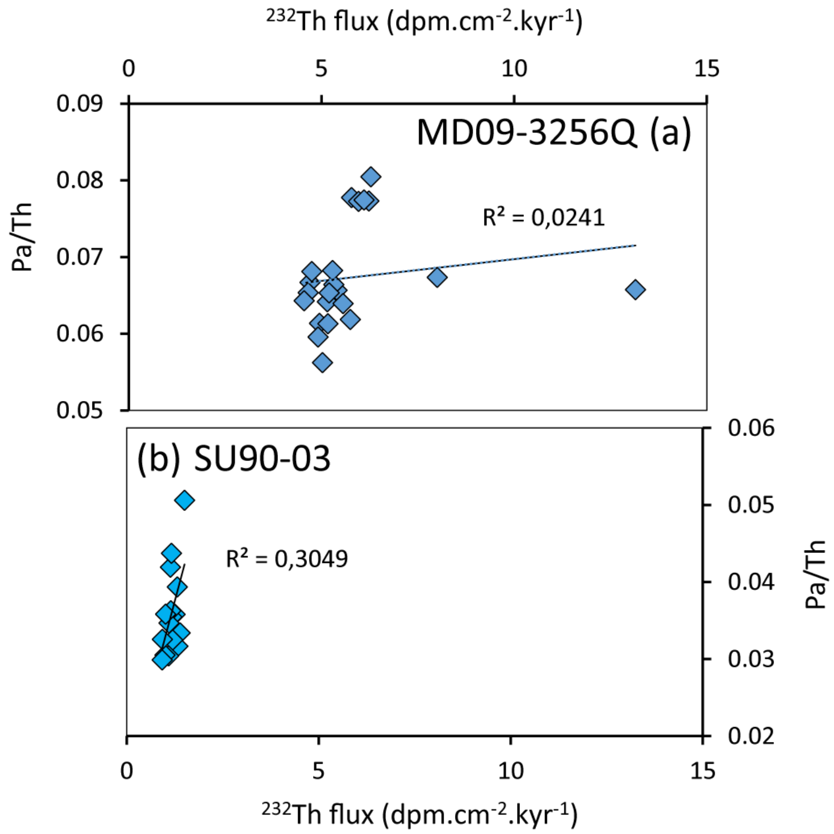

Figure S5: Correlation between the ^{232}Th flux and sedimentary Pa/Th ratio in (a) core MD09-3256Q, (b) SU90-03.

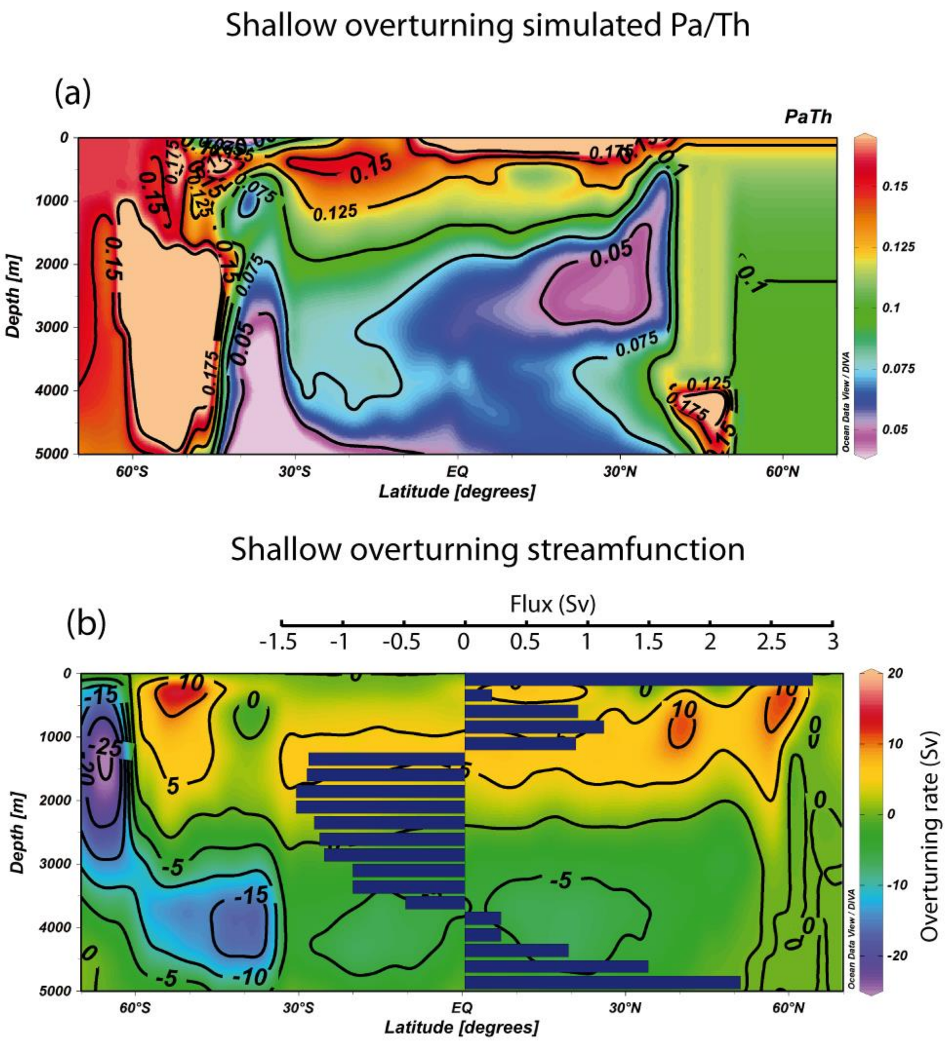

Figure S6: ~~HS1~~ Shallow overturning simulated streamfunction and sedimentary Pa/Th. (a) Simulated sedimentary Pa/Th, (b) simulated streamfunction and flux at the equator (Sv, blue bars, scale on top).

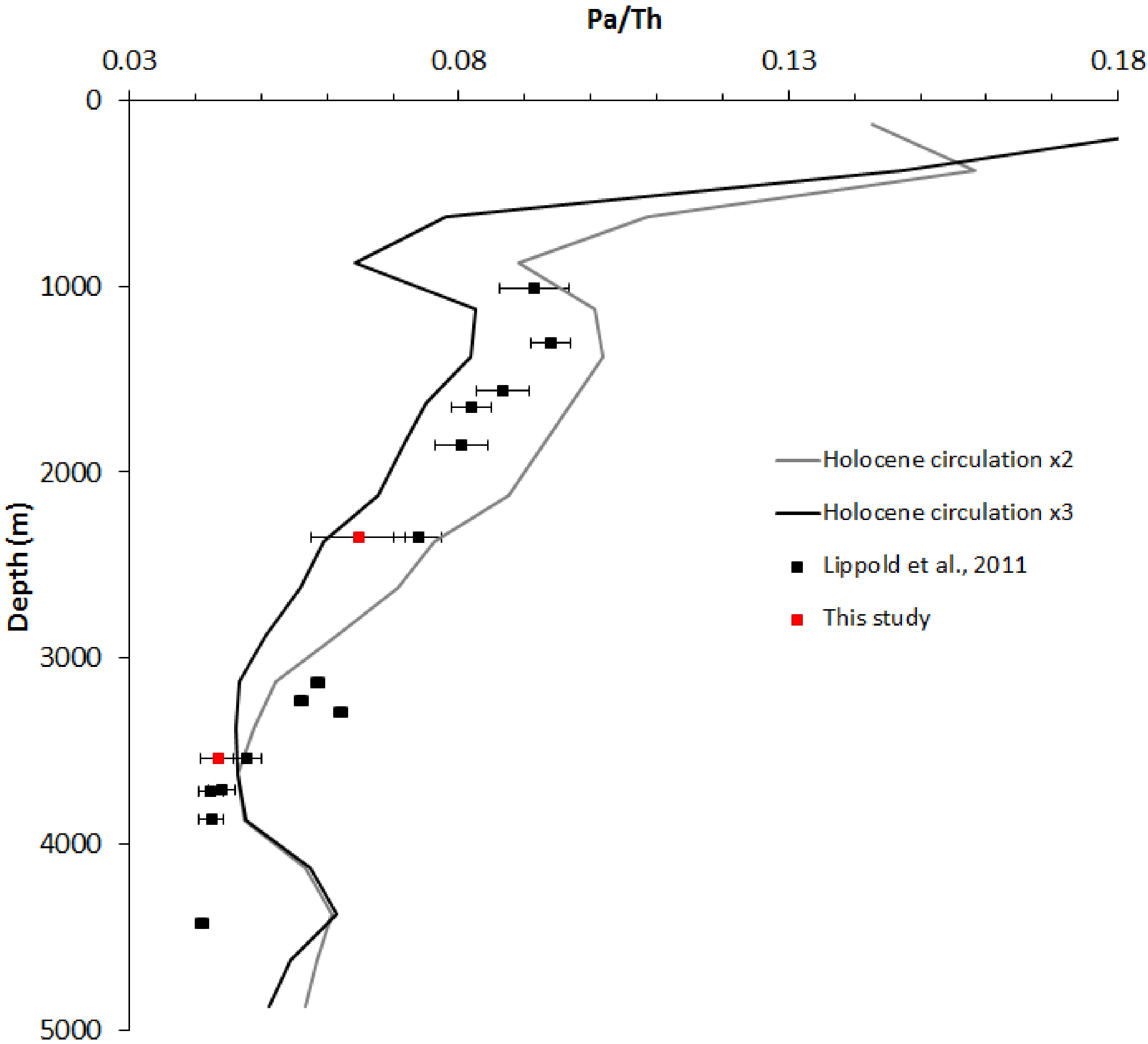

5 Figure S7: Pa/Th on the Brazilian margin. Red squares are data obtained from Holocene sediments in this study. Black squares are data obtained from Holocene sediments in (Lippold et al., 2011). Grey and black lines are simulated Pa/Th values with the 2 and 3x increased Holocene streamfunction respectively. Error bars are 2 sigma.

Table S1: Core locations and age model references.

Core names	Latitude	Longitude	Depth (m)	Age model
MD09-3256Q	03°32.81'S	35°23.11'W	3537	This study
MD09-3257	04°14.69'S	36°21.18'W	2344	(Burckel et al., 2015)
GeoB3910	04°14.7'S	36°20.7'W	2362	(Burckel et al., 2015)
SU90-03	40°30.3'N	32°3.198'W	2475	(Chapman et al., 2000) ^{14}C dates converted to Marine13
ODP 1063	33°41'N	57°37'W	4584	(Böhm et al., 2015)
MD02-2594	34°43'S	17°20'E	2440	(Martínez-Méndez et al., 2010) ^{14}C dates converted to Marine13
V29-172	33°42'N	29°22.98'W	3457	(Bradtmiller et al., 2014)

Table S2: Core MD09-3256Q age model. ^{14}C ages are measured on planktic foraminifer *G. ruber* (white) and converted to calendar ages using the Marine13 curve (Reimer et al., 2013) with no additional reservoir age correction. * Tie points correlating core MD09-3256Q Ti/Ca to GeoB3910 Ti/Ca.

	Depth (m)	Age 14C (kyr)	1σ	Age (Cal kyr)	1σ
	0.040	2.32	0.03	1.93	0.04
	0.070	3.46	0.03	3.34	0.04
	0.200	8.575	0.035	9.22	0.07
	0.420	12.79	0.05	14.41	0.18
	0.580	15.97	0.06	18.82	0.06
	0.660	17.72	0.06	20.88	0.11
	0.880	20.5	0.08	24.16	0.12
	0.920	21.41	0.08	25.36	0.12
	0.960	22.87	0.08	26.79	0.18
	1.150	27.69	0.21	31.19	0.13
	1.270	29.85	0.27	33.65	0.25
*	1.585	/		39.03	0.65
*	1.945	/		47.91	0.62

Table S3: Pa/Th for each time slice in the different cores. Uncertainties are calculated as specified in Sect. S2.

	HS2	1 σ	GI-3	1 σ	GI -8	1 σ	GI-10	1 σ
MD09-3256Q	0.067	0.005	0.064	0.004	0.064	0.006	0.059	0.005
MD09-3257	0.102	0.011	0.072	0.009	0.066	0.010	0.075	0.009
SU90-03	0.033	0.002	0.038	0.04	0.037	0.009	0.040	0.015
ODP1063	0.079	0.007	0.068	0.006	0.071	0.016	na	na
MD02-2594	na	na	0.046	0.005	0.049	0.005	0.049	0.004
V29-172	na	na	0.040	0.002	na	na	na	na

Table S4: Euclidean distance between simulated and measured Pa/Th values in all Atlantic cores for the different times slices. Streamfunctions are multiplied by factors of 1, 2 and 3, where 1 means no change in the streamfunction simulated by the iLOVECLIM model. For each time slice, the best fit between modeled and measured Pa/Th data is displayed in bold.

	HS2	1 σ	GI-3	1 σ	GI -8	1 σ	GI-10	1 σ
~~HS1~~ Shallow x1	0.089	0.005	0.091	0.004	0.081	0.009	0.078	0.014
Shallow ~~HS1~~ x2	0.100	0.006	0.100	0.004	0.080	0.009	0.079	0.014
Shallow ~~HS1~~ x3	0.107	0.007	0.102	0.004	0.085	0.010	0.083	0.014
off mode x1	0.121	0.003	0.162	0.004	0.132	0.010	0.123	0.013
off mode x2	0.133	0.003	0.163	0.005	0.145	0.009	0.138	0.013
off mode x3	0.111	0.003	0.132	0.005	0.123	0.009	0.117	0.013
Holocene x1	**0.039**	0.004	0.060	0.006	0.061	0.008	0.054	0.009
Holocene x2	**0.047**	0.007	**0.044**	0.004	**0.041**	0.008	**0.035**	0.011
Holocene x3	0.059	0.009	**0.049**	0.004	**0.038**	0.010	**0.033**	0.012

Table S5: Euclidean distances between simulated and measured Pa/Th values in all Atlantic cores, not considering the intermediate and deep mid-latitude North Atlantic cores SU90-03 and V29-172, for the different times slices.

	HS2	1 σ	GI-3	1 σ	GI -8	1 σ	GI-10	1 σ
Shallow ~~HS1~~ x1	**0.034**	0.011	**0.025**	0.005	**0.021**	0.008	**0.023**	0.005
Shallow ~~HS1~~ x2	0.057	0.011	**0.025**	0.008	**0.020**	0.010	**0.027**	0.009
Shallow ~~HS1~~ x3	0.067	0.010	**0.037**	0.008	**0.034**	0.010	0.037	0.008
off mode x1	0.046	0.007	0.076	0.007	0.077	0.010	0.065	0.007
off mode x2	**0.033**	0.010	0.070	0.008	0.074	0.009	0.066	0.008
off mode x3	**0.028**	0.010	0.064	0.008	0.068	0.009	0.060	0.008
Holocene x1	**0.019**	0.007	0.052	0.006	0.054	0.008	0.047	0.006
Holocene x2	**0.034**	0.009	**0.032**	0.005	**0.030**	0.007	**0.025**	0.004
Holocene x3	0.048	0.010	**0.030**	0.006	**0.025**	0.011	**0.021**	0.007

Table S6: Opal data in cores SU90-03 and MD09-3256Q.

Core	Depth (cm)	Age (ka)	Opal (wt%)	Opal flux ($g.cm^{-2}.kyrs^{-1}$)
SU90-03	133	26.328	6.7	0.103
SU90-03	145	28.454	5.8	0.081
SU90-03	180	34.247	3.9	0.055
SU90-03	185	35.599	3.7	0.054
SU90-03	190	37.190	2.6	0.036
SU90-03	195	38.780	2.5	0.037
SU90-03	200	39.942	3.0	0.047
SU90-03	205	40.868	3.2	0.050
SU90-03	210	41.713	3.1	0.044
SU90-03	215	42.558	3.3	0.046

MD09-3256Q	146	36.893	0.7	0.020
MD09-3256Q	150	37.576	0.7	0.020
MD09-3256Q	159	39.149	0.7	0.015
MD09-3256Q	159	39.149	0.7	0.015
MD09-3256Q	164	40.382	0.4	0.011

Table S7: Pa/Th and isotopic concentrations ($dpm.g^{-1}$) in core MD09-3256Q. Pa/Th values are computed using a $^{238}U/^{232}Th$ lithogenic correction of 0.5 ± 0.1. 0.5 ky uncertainty was attributed to the core top extrapolated age.

Depth (m)	Age (Cal kyr BP)	1 σ	231Pa	1 SE	230Th	1 SE	232Th	1 SE	238U	1 SE	Pa/Th	1 SE
0	0.05	0.50	0.240	0.001	5.49	0.04	1.190	0.008	1.079	0.006	0.043	0.002
0	0.05	0.50	0.240	0.002	5.51	0.03	1.198	0.007	1.075	0.005	0.043	0.002
0.88	24.16	0.12	0.181	0.002	3.76	0.02	3.460	0.017	1.904	0.006	0.066	0.012
0.89	24.46	0.12	0.241	0.003	4.91	0.02	3.393	0.015	1.802	0.006	0.067	0.008
0.9	24.76	0.12	0.246	0.003	5.08	0.03	2.760	0.014	1.344	0.004	0.066	0.005
0.9	24.76	0.12	0.245	0.003	5.13	0.03	2.641	0.013	1.332	0.004	0.065	0.005
0.92	25.36	0.12	0.259	0.003	5.35	0.03	2.565	0.014	1.253	0.004	0.067	0.005
0.94	26.08	0.15	0.267	0.003	5.44	0.03	2.632	0.015	1.380	0.004	0.068	0.005
0.96	26.79	0.18	0.254	0.003	5.37	0.03	2.558	0.014	1.430	0.004	0.065	0.005
0.98	27.25	0.17	0.241	0.003	5.19	0.03	2.447	0.010	1.312	0.005	0.064	0.004
1.46	36.89	0.49	0.151	0.002	3.41	0.02	1.904	0.012	1.130	0.008	0.066	0.006
1.48	37.23	0.51	0.152	0.002	3.55	0.03	1.947	0.013	1.122	0.007	0.064	0.005
1.5	37.58	0.54	0.150	0.002	3.59	0.03	2.145	0.013	1.394	0.007	0.061	0.006
1.5	37.58	0.54	0.152	0.002	3.53	0.02	2.004	0.012	1.367	0.008	0.063	0.006
1.51	37.75	0.55	0.160	0.002	3.63	0.03	2.024	0.013	1.602	0.011	0.064	0.006
1.56	38.60	0.61	0.226	0.003	4.55	0.03	2.595	0.016	2.117	0.011	0.078	0.007
1.57	38.77	0.63	0.233	0.003	4.81	0.02	2.913	0.012	1.820	0.006	0.077	0.007
1.58	38.94	0.64	0.232	0.003	4.81	0.03	3.040	0.016	1.746	0.006	0.078	0.007
1.59	39.15	0.64	0.235	0.003	4.66	0.04	2.948	0.021	1.645	0.009	0.083	0.007
1.59	39.15	0.64	0.213	0.003	4.67	0.03	2.888	0.017	1.637	0.008	0.072	0.007
1.6	39.40	0.64	0.230	0.003	4.70	0.03	3.050	0.012	1.491	0.005	0.081	0.007
1.61	39.64	0.64	0.186	0.002	4.26	0.03	2.444	0.012	1.265	0.004	0.068	0.006
1.62	39.89	0.64	0.176	0.002	4.13	0.02	2.327	0.010	1.289	0.004	0.065	0.006
1.63	40.14	0.64	0.155	0.002	3.80	0.02	2.042	0.012	1.272	0.007	0.061	0.005
1.64	40.38	0.64	0.150	0.002	3.74	0.02	2.003	0.011	1.247	0.008	0.059	0.005
1.66	40.87	0.64	0.146	0.002	3.76	0.03	2.038	0.014	1.352	0.007	0.056	0.005
1.68	41.37	0.64	0.148	0.002	3.66	0.02	2.057	0.012	1.210	0.006	0.061	0.006

Table S8: Pa/Th and isotopic concentrations ($dpm.g^{-1}$) in core SU90-03. Pa/Th values are computed using a $^{238}U/^{232}Th$ lithogenic correction of 0.5 ± 0.1. 1 ky uncertainty was attributed to extrapolated ages (lower part of the core below 2.09 m, Chapman et al., 2000).

Depth (m)	Age (Cal kyr BP)	1 σ	231Pa	1 SE	230Th	1 SE	232Th	1 SE	238U	1 SE	Pa/Th	1 SE
1.27	24.534	0.148	0.138	0.001	4.07	0.06	0.784	0.004	2.113	0.005	0.036	0.002
1.31	25.832	0.155	0.132	0.002	4.10	0.04	0.870	0.007	2.083	0.016	0.033	0.002
1.33	26.328	0.153	0.130	0.002	4.23	0.07	0.873	0.009	2.038	0.014	0.032	0.002
1.35	26.670	0.147	0.147	0.002	4.59	0.05	0.902	0.010	2.066	0.015	0.035	0.002
1.35	26.670	0.147	0.151	0.001	4.55	0.07	0.789	0.004	2.143	0.005	0.036	0.001
1.39	27.354	0.133	0.168	0.001	4.54	0.05	0.809	0.004	2.352	0.005	0.042	0.002
1.43	28.075	0.129	0.148	0.002	4.43	0.05	0.799	0.004	2.233	0.005	0.036	0.002
1.45	28.454	0.131	0.144	0.001	4.47	0.05	0.781	0.004	2.178	0.005	0.035	0.001
1.47	28.833	0.133	0.129	0.001	4.19	0.06	0.796	0.004	1.980	0.004	0.032	0.001
1.8	34.247	0.341	0.125	0.001	4.32	0.04	0.776	0.004	1.977	0.004	0.030	0.002
1.85	35.599	0.394	0.123	0.002	4.04	0.04	0.699	0.004	1.583	0.003	0.036	0.002
1.9	37.190	0.445	0.107	0.001	4.06	0.04	0.715	0.004	1.354	0.003	0.031	0.001
1.95	38.780	0.497	0.126	0.002	3.82	0.04	0.786	0.004	1.250	0.003	0.044	0.002
2	39.942	0.534	0.102	0.002	3.46	0.05	0.829	0.004	0.888	0.002	0.039	0.002
2.05	40.868	0.523	0.119	0.002	3.46	0.05	0.954	0.005	0.766	0.002	0.051	0.003
2.1	41.713	1.000	0.092	0.001	3.72	0.05	0.660	0.003	0.845	0.002	0.033	0.002
2.15	42.558	1.000	0.098	0.002	3.87	0.05	0.660	0.003	1.272	0.003	0.030	0.002

Table S9: Core MD09-3256Q $\delta^{13}C$ (*C. wuellerstorfi*)

Age (Cal kyr BP)	Depth (m)	$\partial^{13}C$ (‰)	Age (Cal kyr BP)	Depth (m)	$\partial^{13}C$ (‰)	Age (Cal kyr BP)	Depth (m)	$\partial^{13}C$ (‰)
0.52	0.01	1.13	27.48	0.99	0.20	36.21	1.42	0.51
1.46	0.03	1.38	27.71	1	0.07	36.38	1.43	0.67
1.93	0.04	1.29	27.95	1.01	0.29	36.55	1.44	0.65
1.93	0.04	1.33	27.95	1.01	0.08	36.72	1.45	0.86
2.40	0.05	1.28	28.18	1.02	0.25	36.89	1.46	0.96
2.87	0.06	1.28	28.41	1.03	0.33	37.06	1.47	0.40
3.34	0.07	1.36	28.64	1.04	0.15	37.23	1.48	0.55
3.80	0.08	1.34	28.87	1.05	0.38	37.40	1.49	0.42
20.11	0.63	0.23	29.11	1.06	0.40	37.40	1.49	0.59
20.36	0.64	0.30	29.34	1.07	0.45	37.58	1.5	0.68
20.36	0.64	0.21	29.34	1.07	0.08	37.75	1.51	0.53
20.62	0.65	0.31	29.57	1.08	0.34	37.92	1.52	0.44
20.88	0.66	0.23	29.57	1.08	0.37	38.09	1.53	0.19
21.03	0.67	0.09	30.03	1.1	0.48	38.26	1.54	0.40
21.18	0.68	0.12	30.27	1.11	0.50	38.43	1.55	0.71
21.33	0.69	0.31	30.50	1.12	0.45	38.60	1.56	0.26
21.33	0.69	0.33	30.73	1.13	0.33	38.77	1.57	0.43
21.48	0.7	0.29	30.96	1.14	0.35	38.94	1.58	0.22
21.77	0.72	0.03	31.19	1.15	0.36	39.15	1.59	0.22
21.77	0.72	0.36	31.40	1.16	0.68	39.40	1.6	0.40
21.92	0.73	0.25	31.60	1.17	0.58	39.64	1.61	0.31
22.07	0.74	0.32	31.60	1.17	0.42	39.89	1.62	0.29
22.22	0.75	0.16	31.81	1.18	0.25	39.89	1.62	0.21
22.37	0.76	0.17	32.01	1.19	0.71	40.14	1.63	0.30
22.37	0.76	0.25	32.22	1.2	0.62	40.38	1.64	0.38
22.52	0.77	0.29	32.42	1.21	0.25	40.63	1.65	0.52
22.67	0.78	0.31	32.63	1.22	0.33	40.63	1.65	0.27
22.82	0.79	0.30	32.83	1.23	0.56	40.87	1.66	0.13
22.82	0.79	0.18	33.04	1.24	0.68	41.12	1.67	0.57
22.97	0.8	0.24	33.24	1.25	0.56	41.12	1.67	0.33
23.12	0.81	0.21	33.45	1.26	0.70	41.37	1.68	0.80
23.27	0.82	0.08	33.45	1.26	0.50	41.37	1.68	0.71
23.27	0.82	0.09	33.65	1.27	0.83	41.61	1.69	0.41
23.41	0.83	0.16	33.82	1.28	0.41	41.61	1.69	0.55
23.56	0.84	0.12	33.82	1.28	0.53	41.86	1.7	0.88
23.71	0.85	0.02	33.82	1.28	0.58	41.86	1.7	0.77
23.86	0.86	-0.03	33.99	1.29	0.56	42.35	1.72	0.28
24.01	0.87	0.25	34.16	1.3	0.48	42.35	1.72	1.20
24.16	0.88	0.30	34.33	1.31	0.53	42.85	1.74	0.98
24.16	0.88	0.14	34.50	1.32	0.17	43.34	1.76	0.80
24.16	0.88	0.08	34.68	1.33	0.40	43.83	1.78	0.73
24.46	0.89	-0.16	34.85	1.34	0.77	43.83	1.78	0.56
25.06	0.91	0.34	35.02	1.35	0.68	44.33	1.8	0.33
25.36	0.92	0.10	35.19	1.36	0.40	44.33	1.8	0.70
25.72	0.93	0.12	35.36	1.37	0.56			
26.08	0.94	0.39	35.36	1.37	0.49			
26.43	0.95	0.31	35.53	1.38	0.42			
26.79	0.96	0.23	35.70	1.39	0.56			
27.02	0.97	0.39	35.87	1.4	0.43			
27.25	0.98	0.44	36.04	1.41	0.55			

Additional references

Böhm, E., Lippold, J., Gutjahr, M., Frank, M., Blaser, P., Antz, B., Fohlmeister, J., Frank, N., Andersen, M. B. and Deininger, M.: Strong and deep Atlantic meridional overturning circulation during the last glacial cycle, Nature, 517(7532), 73–76 [online] Available from: http://dx.doi.org/10.1038/nature14059, 2015.

Bradtmiller, L. I., McManus, J. F. and Robinson, L. F.: 231Pa/230Th evidence for a weakened but persistent Atlantic meridional overturning circulation during Heinrich Stadial 1, Nat. Commun., 5, 5817, doi:10.1038/ncomms6817, 2014.

Burckel, P., Waelbroeck, C., Gherardi, J. M., Pichat, S., Arz, H., Lippold, J., Dokken, T. and Thil, F.: Atlantic Ocean circulation changes preceded millennial tropical South America rainfall events during the last glacial, Geophys. Res. Lett., 42(2), 411–418, doi:10.1002/2014GL062512, 2015.

Chapman, M. R., Shackleton, N. J. and Duplessy, J.-C.: Sea surface temperature variability during the last glacial–interglacial cycle: assessing the magnitude and pattern of climate change in the North Atlantic, Palaeogeogr. Palaeoclimatol. Palaeoecol., 157(1–2), 1–25, doi:http://dx.doi.org/10.1016/S0031-0182(99)00168-6, 2000.

Francois, R.: Paleoflux and Paleocirculation from Sediment 230Th and 231Pa/230Th, in Proxies in Late Cenozoic Paleoceanography, vol. 1, pp. 681–716, Elsevier., 2007.

Lippold, J., Gherardi, J. M. and Luo, Y.: Testing the 231Pa/230Th paleocirculation proxy: A data versus 2D model comparison, Geophys. Res. Lett., 38(20), 1–7, doi:10.1029/2011GL049282, 2011.

Martínez-Méndez, G., Zahn, R., Hall, I. R., Peeters, F. J. C., Pena, L. D., Cacho, I. and Negre, C.: Contrasting multiproxy reconstructions of surface ocean hydrography in the Agulhas Corridor and implications for the Agulhas Leakage during the last 345,000 years, Paleoceanography, 25(4), 1-12, doi:10.1029/2009PA001879, 2010.

Reimer, P. J., Bard, E., Bayliss, A., Beck, J. W., Blackwell, P. G., Ramsey, C. B., Buck, C. E., Cheng, H., Edwards, R. L., Friedrich, M., Grootes, P. M., Guilderson, T. P., Haflidason, H., Hajdas, I., Hatte, C., Heaton, T. J., Hoffmann, D. L., Hogg, A. G., Hughen, K. A., Kaiser, K. F., Kromer, B., Manning, S. W., Niu, M., Reimer, R. W., Richards, D. A., Scott, E. M., Southon, J. R., Staff, R. A., Turney, C. S. M. and van der Plicht, J.: IntCal13 and Marine13 Radiocarbon Age Calibration Curves 0–50,000 years Cal BP, Radiocarbon, 55(4), 1869–1887 [online] Available from: http://apps.webofknowledge.com.biblioplanets.gate.inist.fr/full_record.do?product=UA&search_mode=GeneralSearch&qid=12&SID=R2qElS8CFcTUu7uanDW&page=1&doc=2 (Accessed 1 July 2015), 2013.

Schott, F. a.: The zonal currents and transports at 35°W in the tropical Atlantic, Geophys. Res. Lett., 30(7), 35–38, doi:10.1029/2002GL016849, 2003.